Arabian Journal of Geosciences (2018) 11: 435
https://doi.org/10.1007/s12517-018-3797-7

ORIGINAL PAPER

Developing a seismic source model for the Arabian Plate

I. El-Hussain[1] · Y. Al-Shijbi[1] · A. Deif[1,2] · A. M. E. Mohamed[1,2] · M. Ezzelarab[1,2]

Received: 7 September 2017 / Accepted: 31 July 2018 / Published online: 9 August 2018

Abstract

A seismic source model is developed for the entire Arabian Plate, which has been affected by a number of earthquakes in the past and in recent times. Delineation and characterization of the sources responsible for these seismic activities are crucial inputs for any seismic hazard study. Available earthquake data and installation of local seismic networks in most of the Arabian Plate countries made it feasible to delineate the seismic sources that have a hazardous potential on the region. Boundaries of the seismic zones are essentially identified based upon the seismicity, available data on active faults and their potential to generate effective earthquakes, prevailing focal mechanism, available geophysical maps, and the volcanic activity in the Arabian Shield. Variations in the characteristics given by the above datasets provide the bases for delineating individual seismic zones. The present model consists of 57 seismic zones extending along the Makran Subduction Zone, Zagros Fold-Thrust Belt, Eastern Anatolian Fault, Aqaba-Dead Sea Fault, Red Sea, Gulf of Aden, Owen Fracture Zone, Arabian Intraplate, and a background seismic zone, which models the floating seismicity that is unrelated to any of the distinctly identified seismic zones. The features of the newly developed model make the seismic hazard results likely be more realistic.

Keywords Seismic source model · Arabian Plate · Seismotectonic

Introduction

Seismic source model is the starting point for any seismic hazard analysis, where the investigated area is divided into a number of distinct seismotectonic source zones. Within each seismic zone, the earthquake occurrence is considered to be temporally stationary and spatially homogeneous. Aldama et al. (2009) reviewed the results of the available seismic hazard studies in the United Arab Emirates (Part of the Arabian Plate). They concluded that inappropriate seismic source models lead to erroneous seismic hazard results. Therefore, seismic source models have a great impact on the hazard results, controlling the shape of the expected ground motion maps.

Most of the earthquake activity of the Arabian Plate is confined to its boundaries, where the relative motion between the Arabian Plate and its surroundings takes place. Moreover, less seismic activity (Although effective) is observed away from the plate boundaries along Palmyra, Abdel Aziz-Sinjar area, Oman Mountains, as well as some small to moderate historical and instrumentally recorded earthquakes scattered within the Arabian Peninsula. Intermediate depth earthquakes are recorded in Makran at Cyprus subduction zones. This seismicity emphasizes the necessity for developing an appropriate seismic source model for seismic hazard and risk evaluations.

There is no standard and proven procedure to model the seismic sources as the delineation process is essentially an issue of expert judgment. Although earthquake catalogs are the main inputs for seismic source modeling, they, alone, provide insufficient data to precisely delineate the source zones and should be integrated with additional information related to the earthquake occurrence process (e.g., active faults, dominant tectonic regime, geophysical, and geodetic data).

For seismic hazard assessment, it is preferable to identify each individual active fault of potential hazard on the area of interest. Correlation of the earthquake locations with the recognized active faults is of great importance in delineating seismic sources. Identifying active faulting is a rather difficult task in the Arabian Plate as in many regions the earthquake

✉ A. Deif
adeif@hotmail.com

[1] Earthquake Monitoring Center, Sultan Qaboos University, Muscat, Oman

[2] National Research Institute of Astronomy and Geophysics, Helwan, Cairo, Egypt

occurrence could not be linked to specific active faults due to (1) the Zagros Fold-Thrust Belt being featured with a series of blind thrust faults with no surface trace and thus has imprecise locations (Berberian 1995), (2) the information on active faulting at many areas in the Arabian Plate is sparse, (3) many fault zones are characterized by their finite widths and inclination, and (4) the locations of many earthquakes are associated with some uncertainty. Additional studies are required to provide the necessary parameters to identify the active faults properly (fault delineation, active segments, slip rate, activity rate, fault mechanism, and maximum magnitude). Therefore, the seismic zones in the present study are defined as seismically homogeneous areas rather than line sources. However, active fault maps are available in Iran, southern Turkey, and along the Aqaba-Dead Sea Fault.

The current study interests in developing a seismic source model based upon an up-to-date homogenous catalog compiled for the Arabian Plate, tectonic activity, surface faulting, available focal mechanisms, seismicity rate, slip rate, available geophysical data, available maps of active faults in Iran, southern Turkey and along the Aqaba-Dead Sea Fault, and previous studies. The earthquake catalog used in the current study to analyze the spatial distribution of earthquakes is compiled by Deif et al. (2017). They used different data sources comprising special studies, local, regional, and international databases to compile a homogenous earthquake catalog for the Arabian Plate based upon moment magnitude (Mw). Deif et al. (2017) developed also a special catalog to be used herein for the available focal mechanisms in the Arabian Plate, constituting a total of 1375 focal mechanism solutions between 1907 and 2015.

Although the current model may be influenced by uncertainties due to the limitation in geological, geophysical, and seismological data, we did not define uncertainty estimates. The uncertainty problem in modern probabilistic seismic hazard assessments (PSHA) has been handled applying alternative seismic source models in the framework of the logic-tree approach. Seismic hazard assessment will not be discussed herein, as it is the main target of another future research.

Seismotectonic setting of the Arabian Plate

The Arabian Plate is detaching from the major African Plate since about 25–30 million years due to the strike-slip movement along the Aqaba-Dead Sea Fault (ADSF), the sea floor spreading along the Red Sea-Gulf of Aden axial troughs, and the subduction of Africa and Arabia beneath the Eurasian Plate (Johnson 1998). This system of combined and diverse tectonic movements leads to the rotation of the Arabian Plate toward the north-northeast and formation of ocean spreading along the Red Sea and Gulf of Aden. The convergence of the Arabian Plate toward Eurasia is accommodated along the Makran Subduction Zone, and the Zagros Fold-Thrust Belt up to the East Anatolian Fault in the northwest. To the southeast, the Owen and Murray Fracture Zones separate the Arabian Plate from the Indian Plate (Fig. 1). These tectonic motions are responsible for the relative high seismic activity that affected the boundaries of the Arabian Plate during the recorded history. The interior of the Arabian Plate is considered as a stable continental area because most of the seismic activities are concentrated along its active boundaries (Figs. 2 and 3).

Several studies were carried out to handle the present-day motion of the Arabian Plate relative to its surrounding (e.g., McClusky et al. 2003; Reilinger et al. 2006; ArRajehi et al. 2010). Such studies can be used to interpret the interaction of the Arabian plate with the surroundings, providing their slip rates. The velocity field indicates counterclockwise of the Arabian Plate and its surroundings with motion rates ranging from 20 to 30 mm/year, within the slow-moving Eurasian, Nubian, and Somalian Plates with about 5 mm/year (Reilinger et al. 2006). The interaction of the Arabian plate with the surrounding ones could be represented in Fig. 4, as the vectors proportional to velocities indicate their motion (ArRajehi et al. 2010). Figure 5 depicts the fault plane solution for earthquakes with magnitude ≥ Mw 5.5 between 1907 and 2015 in Arabian Plate. It is evident that large earthquakes have occurred at the pre-defined active tectonic trends and their focal mechanisms are consistent with the regional kinematics. Good agreement between the senses of motion indicated by plate velocities and earthquake mechanisms.

The Makran is a 900-km-long, east-west trending subduction zone, where the bottom of Oman Sea proceeds toward north beneath the Eurasian Plate at a GPS-constrained slip rate ranging from 19.5 ± 2 to 27 ± 2 mm/year (Vernant et al. 2004). The introduction of Makran region as a subduction zone was initially provided by Stoneley (1974). Afterward, Shearman (1977) and Farhoudi and Karig (1977) submitted data supporting this suggestion. The Makran Subduction Zone emerges under Oman Sea at latitude of about 24° N, evolving an extensive north-dipping deformation zone of thrust faults and accompanied folds that strike toward east (Haghipour et al. 1984; Hessami et al. 2003). Available well-constrained fault plane solutions confirm the thrust nature of Makran's faults (Fig. 5).

Zagros-Bitlis Thrust-Fold Belt is a 1500-km-long collision zone between the Arabian and Eurasian plates. It is distinguished by quite high seismic activity, causing seismic hazard to several neighboring nations. It includes a widespread series of thrust faults concealed by thick folded Phanerozoic deposits, and strike-slip faults striking NS oblique to the belt (Berberian 1995), accommodating the deformation within the belt. Using GPS measurements, Reilinger et al. (2006) specified a compression sense of motion along the entire Zagros zone at slip rate of 23 ± 1 mm/year at its southernmost part, with declining amplitude 19 ± 1 mm/year and an intensifying strike-slip motion to the north.

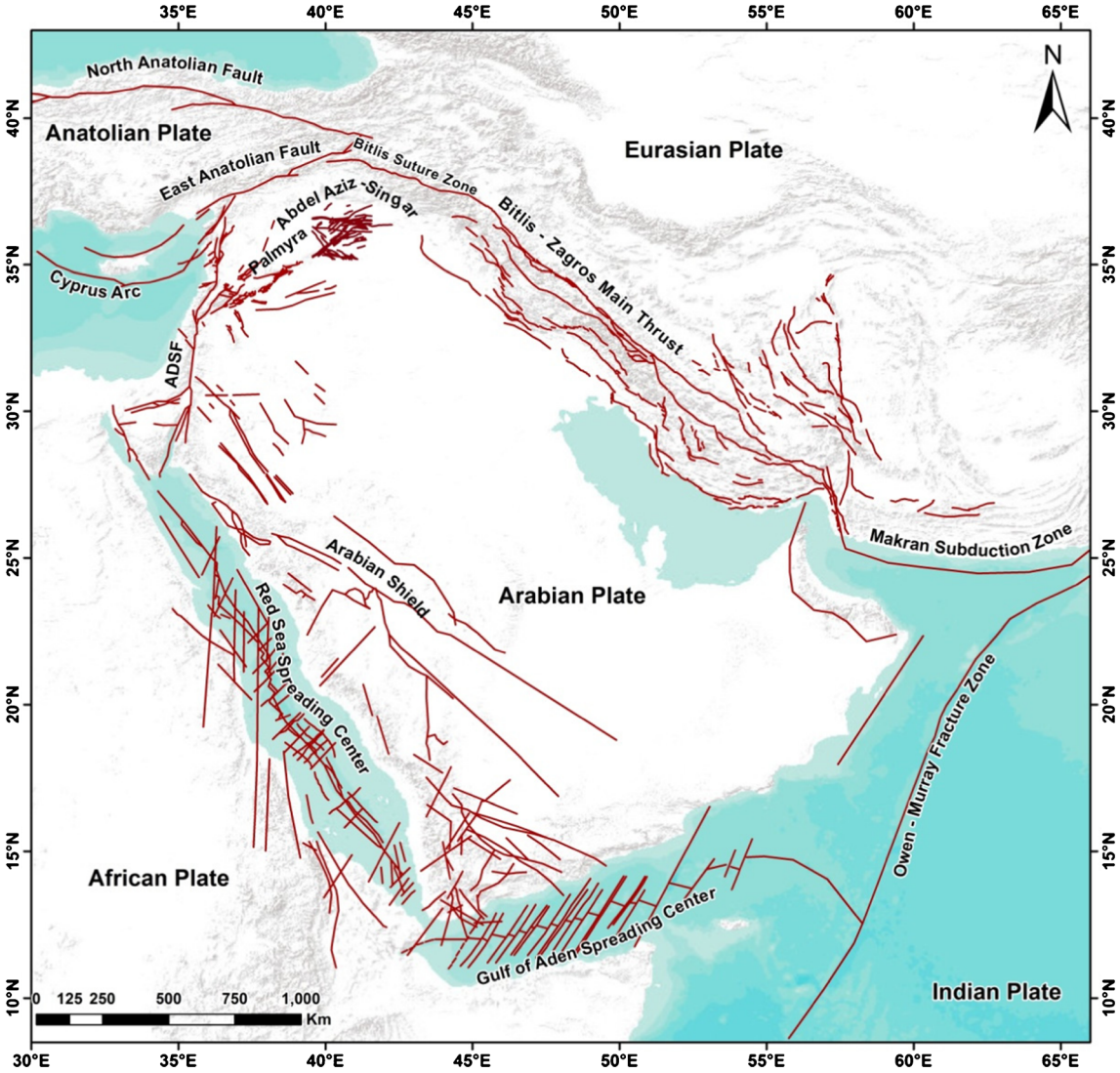

Fig. 1 Tectonic elements of the Arabian Plate (Deif et al. 2017). *ADSF* Aqaba-Dead Sea Fault, compiled from Johnson (1998), Brew (2001), Brew et al. (2001), Gullen et al. (2002), Hessami et al. (2003), Bosworth et al. (2005), and Gomez et al. (2007). Brown lines indicate the faults

The East Anatolian Fault is a left lateral strike-slip plate boundary, detaching the Arabian Plate from the Anatolian Plate. It extends for about 600 km from the Aqaba-Dead Sea Fault toward northeast until it meets the north Anatolian Fault (Fig. 1). The East Anatolian Fault exhibits a predominant left-lateral strike-slip at 9 ± 1 mm/year combined with 3 mm/year dip slip, giving rise to great earthquakes with magnitudes exceed Mw 7.0 (Bulut et al. 2012). Focal mechanism solutions of large earthquake along this active zone support the predicted sense of motion by GPS measurement.

The Aqaba-Dead Sea Fault is a sinistral plate boundary that formed in the Mid-Cenozoic, connecting the Red Sea at the south and the East Anatolian Fault (EAF) to the north. It is one of the rare plate boundaries on the Earth, separating the African from the Arabian Plate and exposed on the continent. Offset markers along the fault reveal a geologic 105 km northward left lateral strike-slip, giving rise to a horizontal slip rate of 5 to 10 mm/year since the Miocene (e.g., Bartov et al. 1980; Sneh 1996). GPS results predict an increasing rate of motion toward north from 5.6 ± 1 mm year^{-1} of pure sinistral motion at the southernmost part of the fault to a combined system of strike and dip motions at a rate of 7.5 ± 1 mm/year to the north. To the north of Lebanon bend, motion is divided between 6 ± 1 mm/year fault parallel and 4 ± 1 mm/year^{-1} fault normal motions (McClusky et al. 2003). Various fault plane solutions characterize the seismicity of the Aqaba-Dead Sea Fault (Fig. 5) but the focal mechanisms of the large earthquakes verify the geological evidences of its sinistral nature (e.g., Salamon et al. 2003; Palano et al. 2013).

The Red Sea runs from 13o to 28o N for about 2000 km long, providing a useful setting to study the growth from continental rifting to oceanic accretion. Geological and geophysical studies provided conclusive evidences confirming the creation of juvenile oceanic crust along several segments of the axial

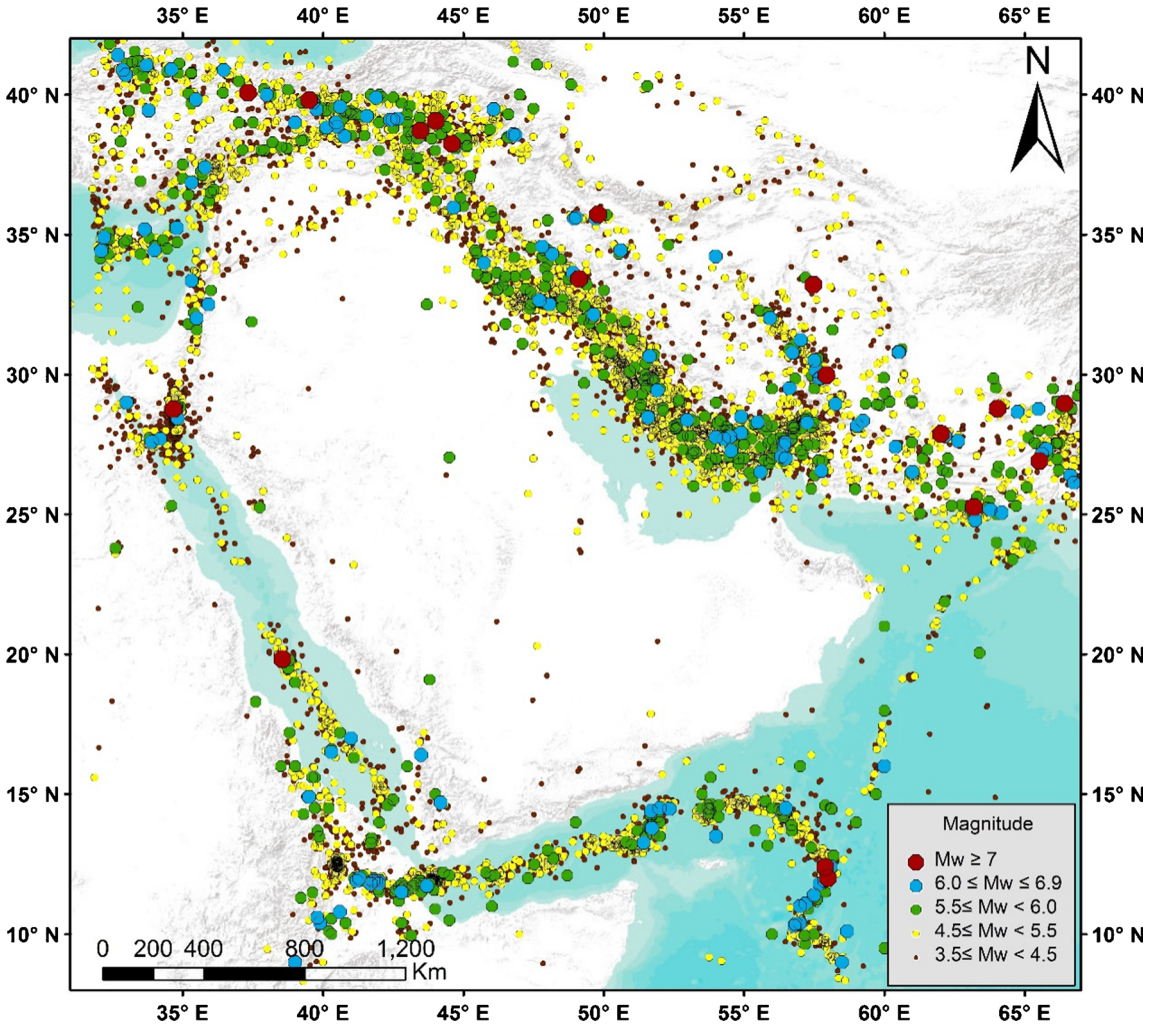

Fig. 2 Epicentral distribution of instrumentally recorded earthquakes of the Arabian Plate from 1900 to 2015 (Deif et al. 2017)

trough (e.g., Girdler and Underwood 1985; Rasul et al. 2015). The oceanic crust that resulted due to the sea floor spreading process is fully identified up to 20° N, instigating the persistent drift of the Arabian Peninsula. The GPS measurements (Fig. 4) imply spreading rates along the Red Sea varying from about 15 ± 1 mm/year at 15° N to 5.6 ± 1 mm/year at the Gulf of Aqaba (ArRajehi et al. 2010). Fault plane solutions in the Red Sea show normal and strike-slip senses of motion, revealing the activity of the axial trough as well as the transform faults perpendicular to it.

The Gulf of Aden is an oblique rift system along the divergent Arabia-Somalia plate boundary, running from the Owen Fracture Zone to the east to the Red Sea to the west (Lorei et al. 2010). The ENE-WSW strike of the Gulf of Aden is oblique to the NE-SW relative motion between the Arabian and African Plates (Fig. 4). Extension of the Gulf of Aden rift system began at 35 Ma due to the northeast detachment of the Arabian plate from the African plate at a rate of about 20 mm/year (ArRajehi et al. 2010). Extension eventually gave way to seafloor spreading at about 18 Ma ago in the eastern part of the Gulf and propagated until terminating at the Afar plume. The spreading center is substantially divided by distinct transform faults due to oblique rifting (e.g., Tamsett and Searle 1990; Bosworth et al. 2005). Fault plane solutions show dominant normal as well as strike-slip.

Owen Fracture Zone is a dextral transform fault stretching along the eastern margin of the Arabian Plate, separating it from the Indian Plate. The Arabian Plate moves a little bit faster than the Indian Plate northward to collide with the southern boundary of the Eurasian Plate. This variation in plate motions is accommodated by the Owen Fracture Zone, which extends for about 1100 km long. This seismic zone is characterized by one of the tiniest relative motion among major tectonic plates globally. DeMets et al. (1990) utilized the azimuths of two transform faults derived from typical sounding profiles and six earthquake slip vectors to conclude a dextral motion of 2 mm year^{-1} along the Owen fracture zone. Fournier et al. (2008) combined three independent databases (multibeam bathymetry, earthquake fault plane solutions, and space geodesy) to predict a present-day motion of about

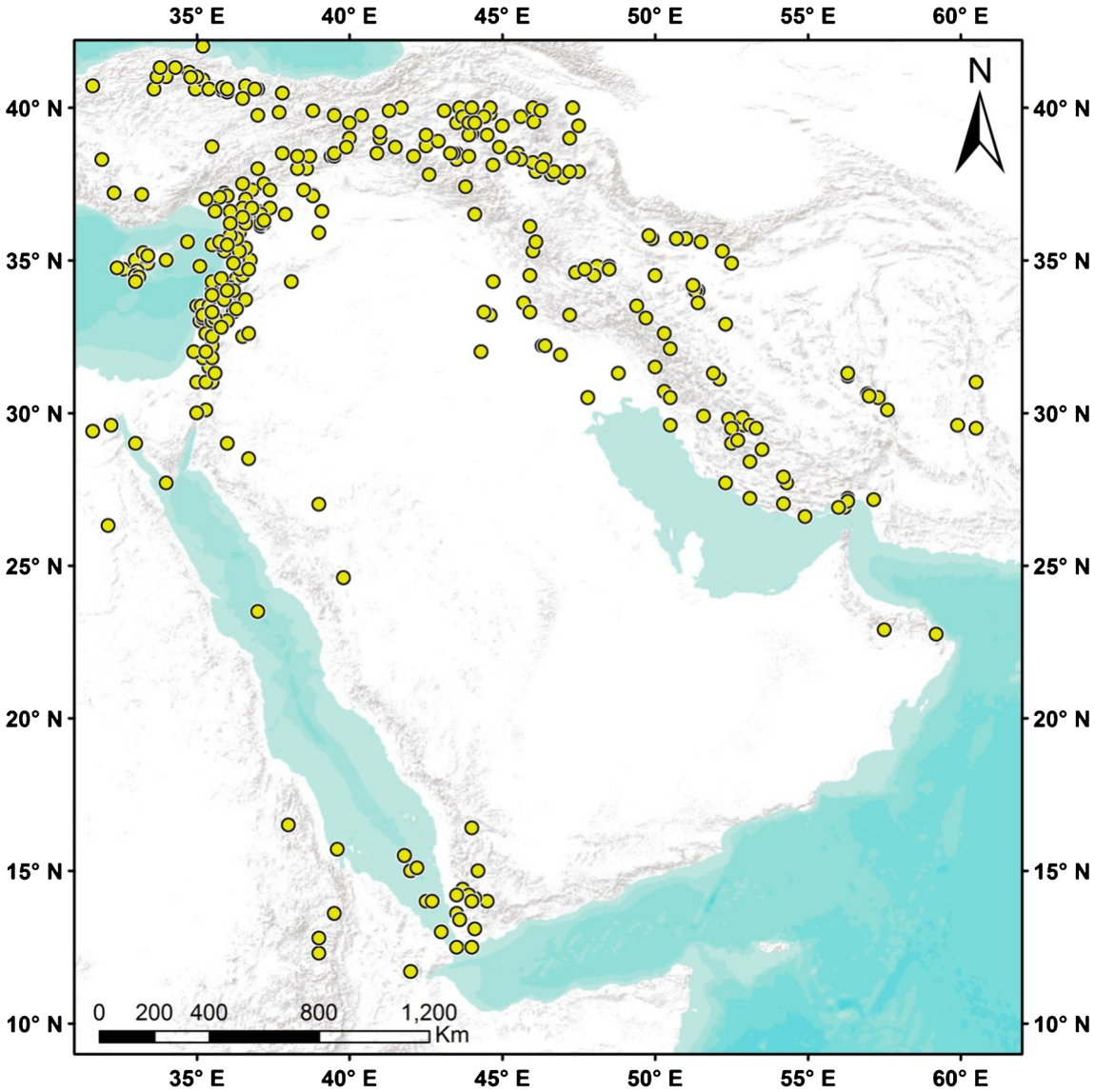

Fig. 3 Historical earthquakes of the Arabian Plate

3 mm/year along this zone. ArRajehi et al. (2010) partitioned the present-day motion along Owen Fracture Zone into 3.2–2.5 ± 0.5 mm/year right lateral, increasing from north to south, and 1–2 mm/year extension. With this very low plate motion rates, the seismicity on these two structures is not expected to be very high. Available focal mechanisms along Owen fracture zone are dominated by dextral faulting, and oblique normal faulting with a dextral component at Murray Ridge.

Details of the developed seismic source model

Fifty-seven seismic source zones, including a background one, were delineated to adequately model the seismotectonic setting of the Arabian Plate (Fig. 6). The seismic source zones were delineated taking into account all possible seismic sources that may affect the Arabian Peninsula, including the Makran Subduction Zone, the Zagros Fold-Thrust Belt, the Eastern Turkey Collision Zone, the Aqaba-Dead Sea Fault, the Red Sea, Yemen, the Gulf of Aden, the Owen Fracture Zone, the Murray Ridge, the Oman Mountains, and the Arabian Shield. More seismic source zones were added to cover the Cyprus, the Palmyride, and neighboring regions. The seismic zones of the Zagros Fold-Thrust Belt, the Makran Subduction Zone, the Gulf of Aden, the Owen Fracture Zone, and the Murray Ridge were delineated and modified mainly based on the work done by El-Hussein et al. (2012). The seismic zones of the Eastern Turkey collision zone were modified after Bayrak et al. (2009). The characteristics of each delineated seismic source zone are briefly discussed as follows:

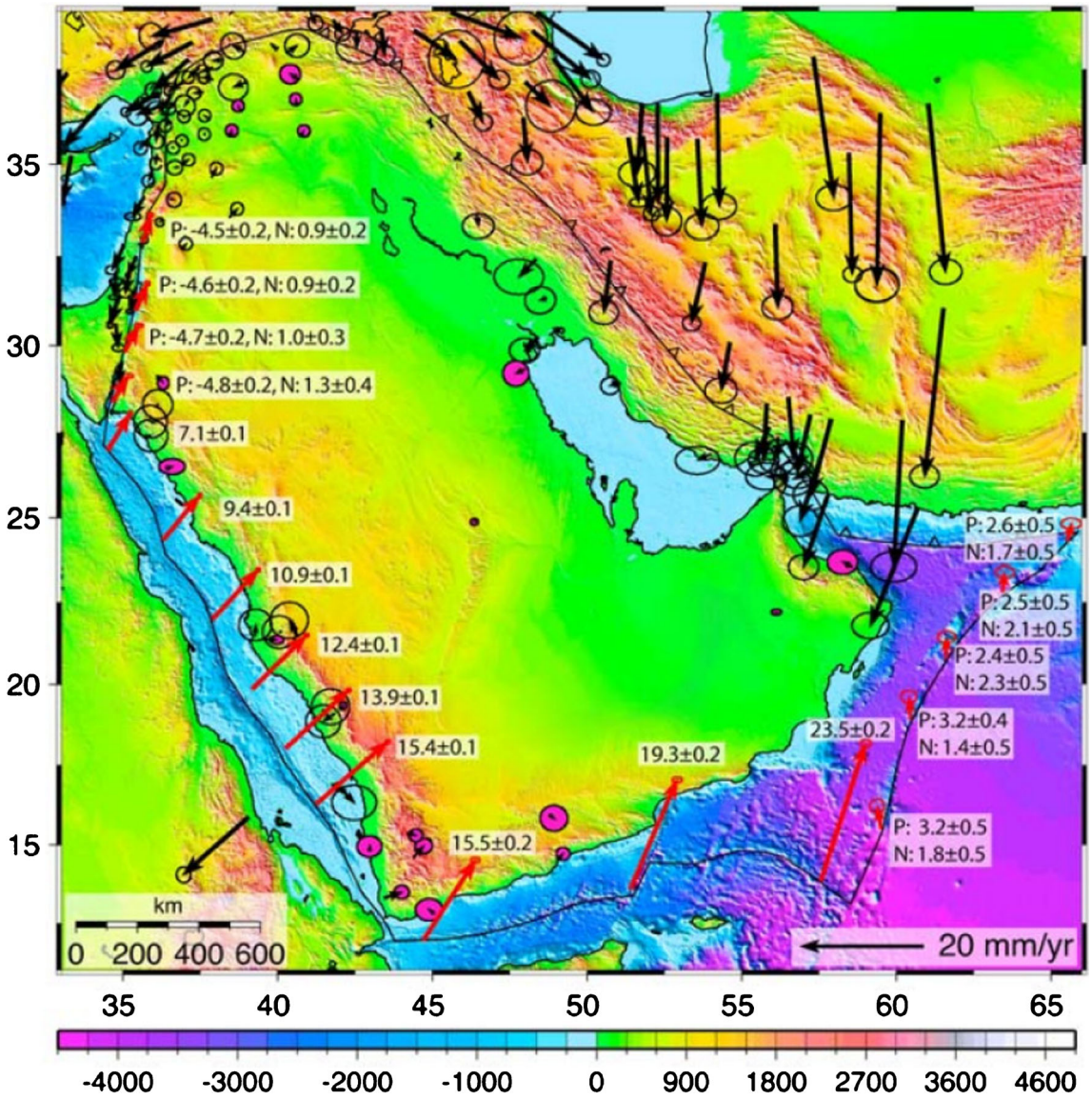

Fig. 4 GPS velocities per year of the Arabian Plate with the vectors are proportional to the velocity of their motion (ArRajehi et al. 2010)

Seismic source zones of the Makran Subduction Zone

The northward Makran Subduction Zone consists of a large sedimentary prism accreted during the Early Cretaceous (Byrne et al. 1992). Aldama (2009) showed that the subducting plate has a dip of about 6° up to latitude 26.5° N, at which the dip becomes steeper, with a dipping angle of about 19°.

Although the seismicity of this zone is low compared with other subduction zones, it has large earthquakes. The largest reported earthquake occurred in 1945, reaching Mw 8.1. It was a tsunamigenic event with a rupture length of about 200 km in the East-West direction (Byrne et al. 1992; Heidarzadeh and Satake 2014). This earthquake was associated with low-angle thrust faulting, causing about 300 fatalities (Ambraseys and Melville 1982). Since 1945, just one large intermediate depth earthquake with Mw 7.8 took place on 16 April 2013 at the Iran and Pakistan borders, showing normal faulting mechanism due to the flexure of Arabian Plate as it subducts beneath Eurasia. Makran subduction zone demonstrated several tsunamigenic events in the last 5000 years using geological and archeological data (Hoffmann et al. 2013). These events exceeded the 1945 earthquake. Faulting in large earthquakes is likely to occur between the surface and about 40 km depth. This zone is also associated with intermediate depth (50 to 150 km) earthquakes, which have mostly normal faulting mechanism. Intermediate depth earthquakes are recorded inland within the down going slab and are modeled as area sources.

Large earthquakes are reported to always occur in the eastern part of the Makran Subduction Zone, suggesting a likely segmentation. Makran segmentation is supported by the offsets in the volcanic arc and the separation of the Lut and

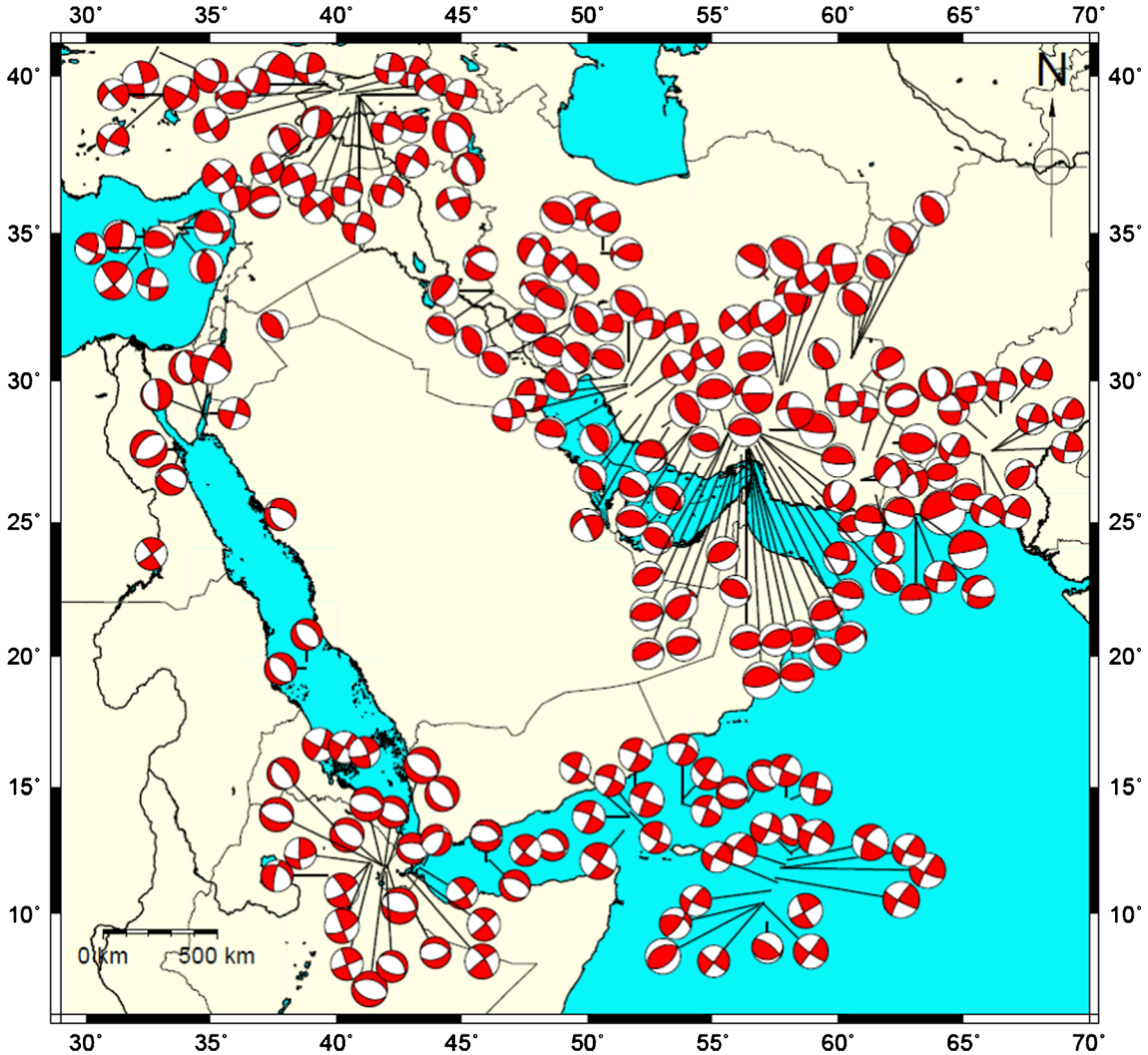

Fig. 5 Fault plane solutions for earthquakes with Mw ≥ 5.5 in the Arabian plate, beach balls red quadrants denote compression and the white ones dilatation (data used from Deif et al. 2017)

Helmand blocks (Fig. 7). On contrary to Ambraseys and Melville (1982), who located 1483 earthquake of Ms 7.8 in the western Makran section, the authors leant to the opinion of Musson (2009), who believes that the western segment of the Makran Subduction Zone is free of large earthquakes and it is unlikely to have a single earthquake rupturing the entire Makran Subduction Zone. The absence of large events in western Makran indicates either totally aseismic subduction or the plate margin is presently locked and waiting for a large earthquake. The presence of raised beaches and mud volcanoes suggest the seismic activity of the western segment do exist (Page et al. 1978; Quittmeyer 1979).

Two seismic regions namely Makran Interplate and Makran Intraplate were principally defined. The boundary between these two regions was delineated at the line where the subducting plate changes its slope, and where the intermediate depth earthquakes are recorded frequently. The Makran interplate region was subdivided into two seismic zones (zones No. 1 and 3) to reflect the variation in seismicity between the eastern and western parts (Fig. 8). The boundary between these two zones is identified near longitude 61° E, in coincidence with the Sistan Suture Zone (Byrne et al. 1992). Similarly, the intraplate region is subdivided into two seismic zones (zones No. 2 and 4) to separate the Jaz Murian depression from the Hamun Mashkel Depression (Figs. 4 and 5).

Seismic zones of Zagros Fold-Thrust Belt

Zagros is a collision zone between the Arabian and the Eurasian Plates. It is characterized by intense seismicity in a belt of 200 to 300 km width, stretching for about 1500 km from the East Anatolian Fault to the Makran Subduction Zone (Fig. 1) (Jackson and McKenzie 1984; Berberian 1995; Hessami et al. 2003). Most earthquakes in this zone are supposed to take place along blind active faults without co-seismic surface rupture (Berberian 1995). The shallow depth, large earthquake

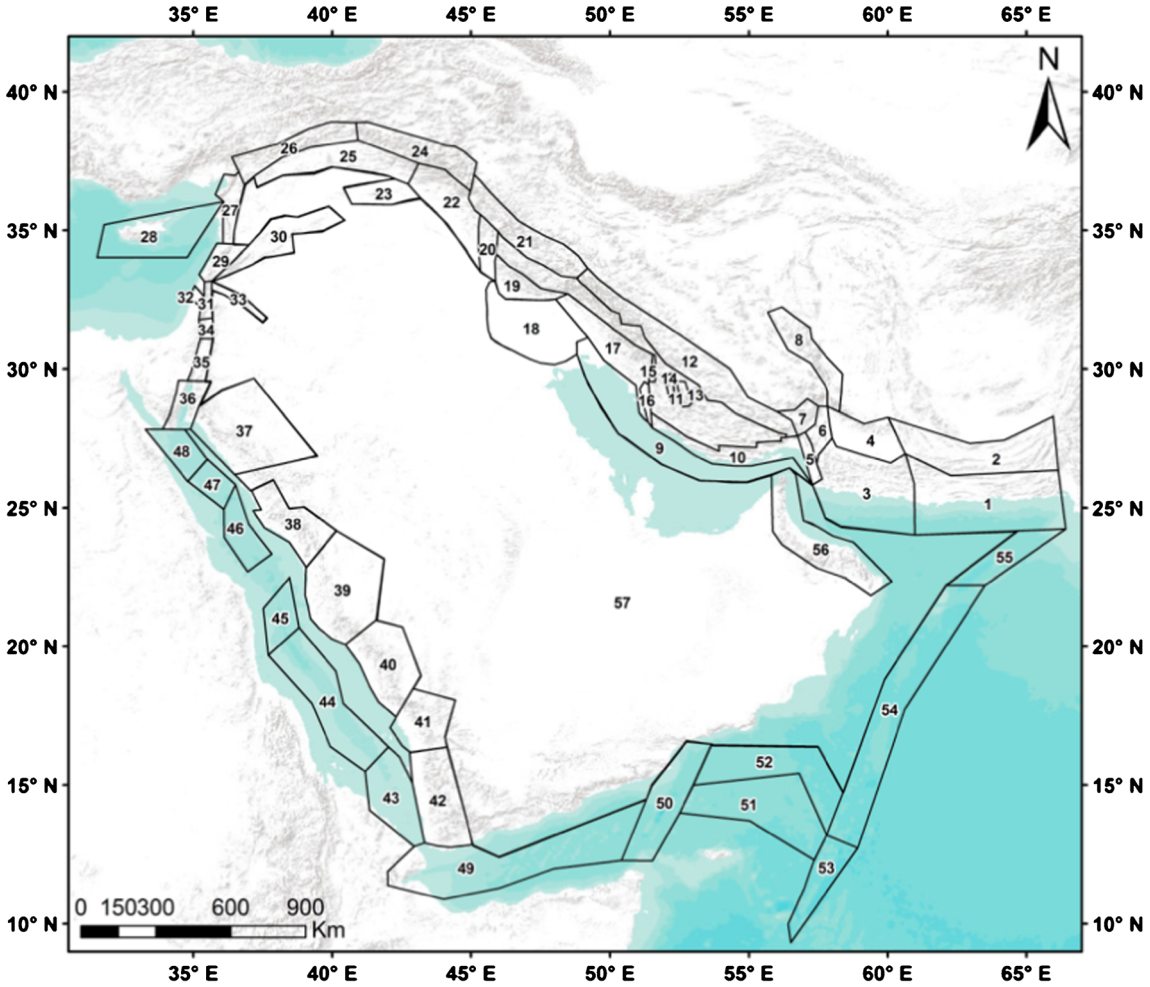

Fig. 6 Developed seismic source model for the Arabian Plate

that struck the Iraqi-Iranian border in November 2017 with Mw 7.3 is not an exception as no surface rupture observed, supporting the blind faults assumption of Berberian 1995.

Earthquakes occur at shallow depths (8–14 km), and are mostly caused by high-angle reverse faulting with dips in the range of 30–60°, a striking parallel to the main trend of the fold-thrust belt at the surface (e.g., Gillard and Wyss 1995; Hessami et al. 2006; Deif and El-Hussain 2012). Some strike-slip earthquakes are present on faults trending NS oblique to the fold belt, accommodating the inner deformation between the northern and central Zagros zones (Deif et al. 2017). There is no historical evidence for great earthquakes in the Zagros Fold-Thrust Belt. Zagros earthquakes rarely exceed a magnitude of 7.0 and most of them are believed to occur without co-seismic surface rupture on the blind active thrust faults (Berberian 1995; Hessami et al. 2003).

Based upon the differences in the seismic activity, active faulting behavior, geomorphological features, and surface geology, the Zagros Fold-Thrust Belt is divided into nine areal seismic zones as well as five seismic zones surrounding four principal strike-slip faults. The nine seismogenic zones are the High Zagros Thrust Belt (zone No. 12), the Simple Fold Belt (zone No. 11), the Zagros Foredeep (zone No. 10), the Arabian Gulf (zone No. 9), the Dezful Embayment (zone No. 17), the Mesopotamia (zone No. 18), the Mountain Front Fault (zone No. 19), the Posht-e Kuh Arc (zone No. 21), and Kirkuk Embayment (zone No. 22) as seen in Fig. 6. The seismic zones associated with the principal strike-slip faults are the Sabz Pushan Fault (zone No. 13), the Karebas Fault (zone No. 14), the Kazerun-Borazjan Fault (zones No. 15 and 16), and the Khanaqin Fault (zone No. 20). Detailed description of each sub-zones will be discussed in the following sections.

The High Zagros Thrust Belt

The High Zagros Thrust Belt (zone No. 12) is a narrow thrust belt of NW-SE trend, comprises highly deformed Mesozoic rock units (Fig. 9). It is limited by the Main Zagros Reverse Fault (MZRF) to the northeast and by the High Zagros Fault (HZF) to the SW. MZRF shows a NW-SE trend from north-western Iran toward Bandar Abbas area (Fig. 10), where it deviates into N-S Zendan-Minab Fault, separating the

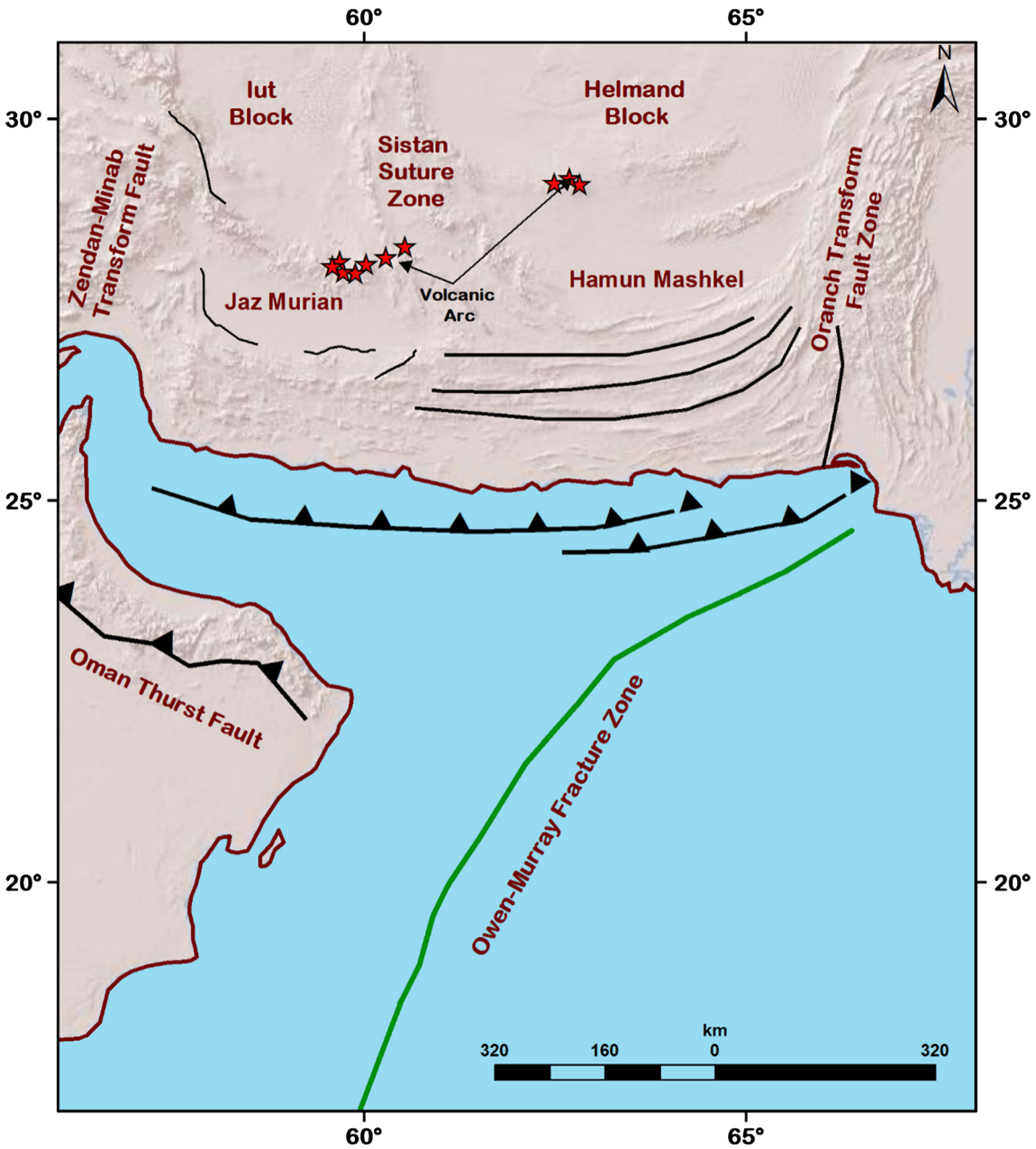

Fig. 7 The tectonic framework of the Makran Subduction Zone and Owen Fracture Zone (Modified after Johnson (1998), Pararas-Carayannis (2004), and Mokhtari et al. (2008))

Zagros Fold-Thrust Belt from the Makran Subduction Zone. The extension of the MZRF northwestward is the Main Recent Fault (MRF), which is a young right lateral fault. Historical and instrumental earthquakes with magnitude greater than 6.0 were reported in this seismic zone.

The Zagros Simple Fold Belt

This seismic zone (zone No. 11) lies between the HZF in the northeast and the Mountain Front Fault (MFF) in the southwest (Fig. 10). It is distinguished by great elongated anticlines (Talebian and Jackson 2004). The Zagros Simple Fold Belt has a variable width along its strike, reaching about 250 km to the southeast and decreases to about 120 km to the northwest (Fig. 9). The thickness of the sedimentary cover in this seismic zone reaches about 12 km (Berberian 1995). This seismic source zone could be considered as one of the most active zones within the Zagros Belt as it contains many of the relatively large earthquakes.

The Zagros Foredeep

The Zagros Foredeep (zone No. 10) is bounded to the northeast by the MFF and to the southwest by the Zagros Foredeep Fault

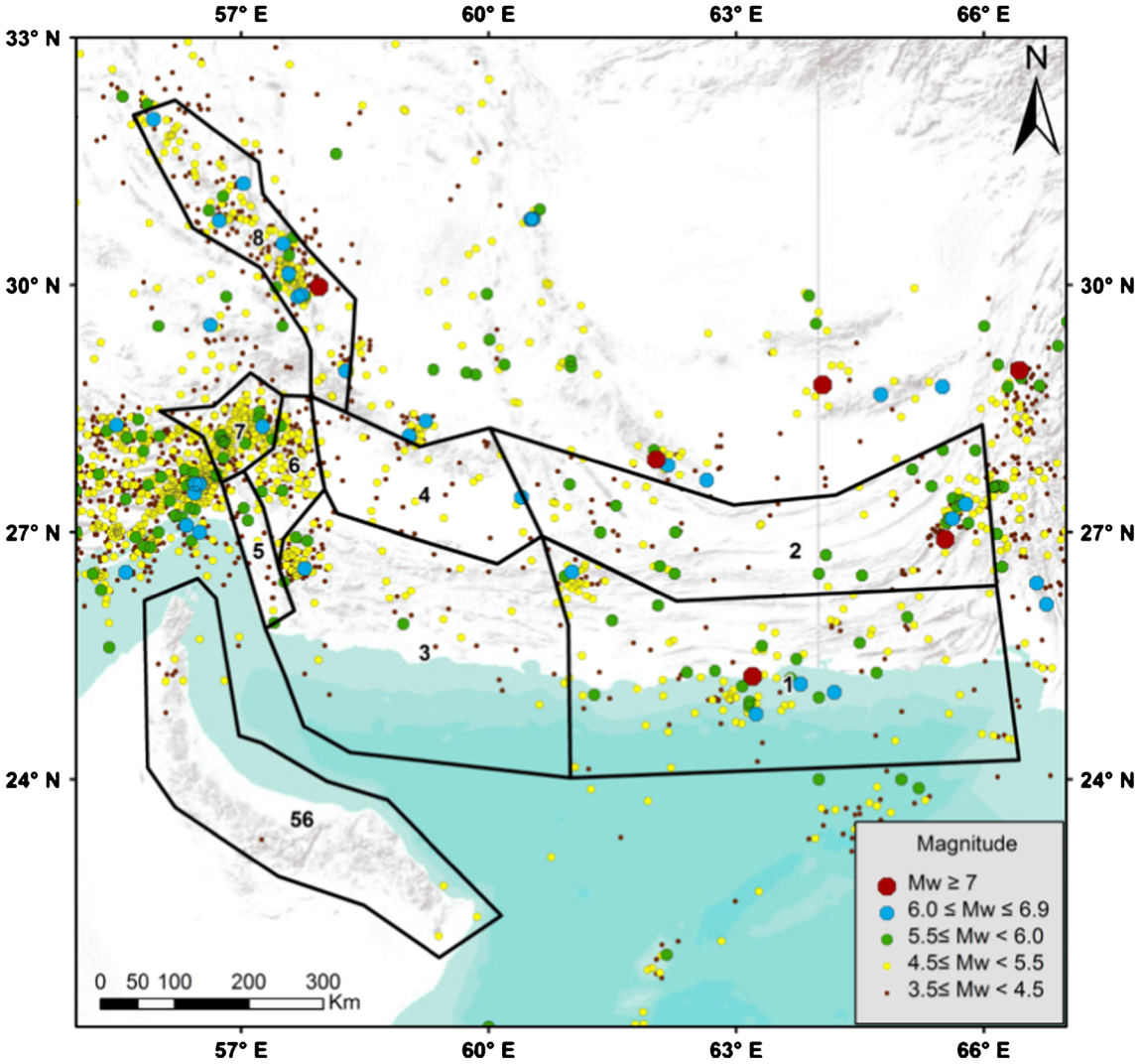

Fig. 8 Seismic source zones of the Makran Subduction Zone (1, 2, 3, 4), transition area between Makran and Zagros, Gowk Fault (5, 6, 7, 8), and Oman Mountains (56)

(ZFF). The MFF consists of fragmented thrust segments of less than 115 km long, so they are not able to produce great earthquakes. The MFF is bounded by the southeastern segment of the HZF in Bandar Abbas area, where the March 21, 1977 event with Mw 6.7 and its aftershocks took place (Fig. 10).

The anticlines of Zagros Foredeep are still rising since the end of the Miocene, as evidenced by unconformities in the Pliocene fresh water sediments and Recent folded gravels (Lees and Falcon 1952; Falcon 1961). The seismic activity reported to the south of ZFF is generated by a similar tectonic process to that in Zagros Foredeep and almost with the same rate. Thus, we expanded the southern boundary of the Zagros Foredeep farther to the south to include this seismicity (Fig. 9).

The Arabian Gulf

The Arabian Gulf (zone No. 9) is a shallow marginal sea of the Indian Ocean with about 900 km long and a width ranging from 115 to 185 km (Fig. 9). It is of a tectonic origin and covers the Arabian shelf platform with average water depth of about 35 m (Berberian 1995). Tectonically, the Arabian Gulf contains the southern border of the Zagros Thrust-Fold Belt, which is defined in the current study by the seismicity in the Gulf. Herein, the seismicity is obvious, although at a lower rate than the Zagros Thrust Belt Zones.

The Dezful Embayment

The Dezful Embayment (Fig. 9), one of the richest oil provinces all over the world, is situated southwest of the MFF. The Dezful Embayment Fault (zone No. 17) marks the northern limit of the Dezful Embayment and is located in the area between the MFF and ZFF. The Kazerun-Borazjan Transverse Fault and the ZFF mark its south-southeast and southwest boundaries, respectively (Fig. 10). The Dezful Embayment (DEF) shows a vertical displacement of more

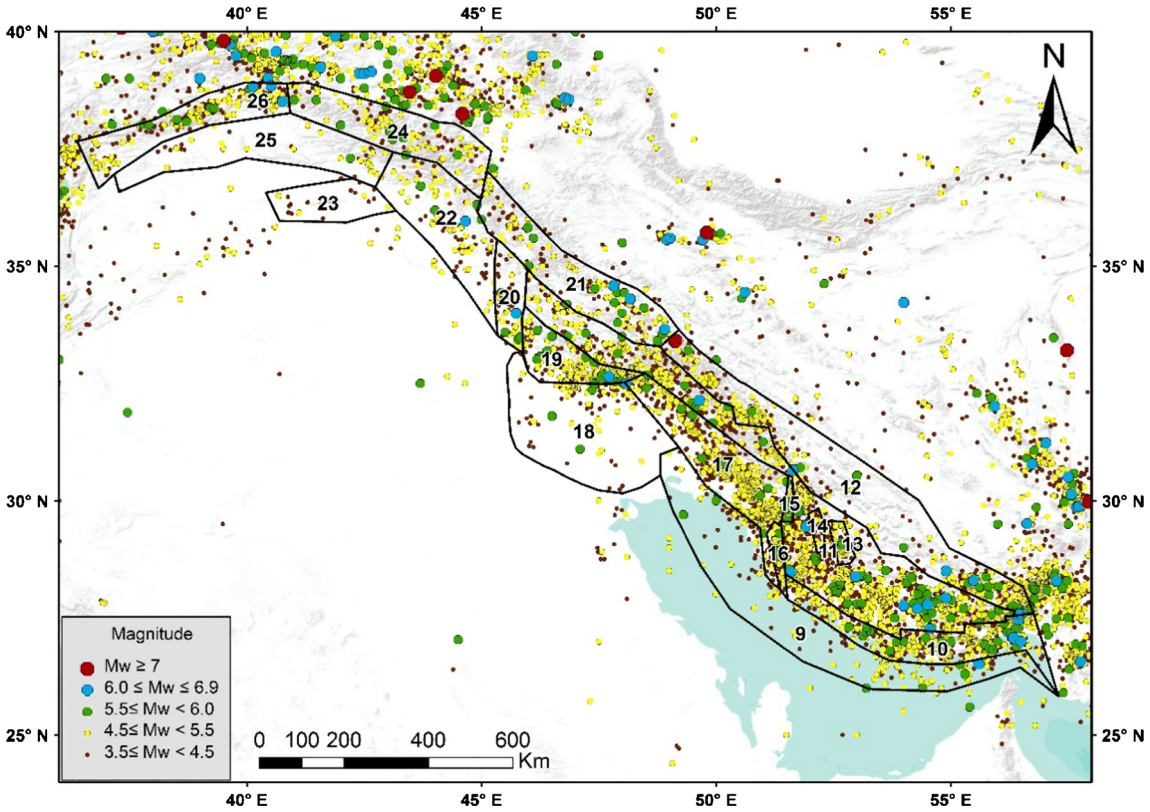

Fig. 9 Detailed seismic source zones and seismicity of the Zagros and the East Anatolian regions

than 3 km (Huber 1977). Two earthquakes, showing thrust mechanism, occurred on June 5, 1977 and on September 18, 1985 with Mw 6.1 and 5.3, respectively, seem to be associated with the DEF (El-Hussain et al. 2010).

The Mesopotamia

The Mesopotamian Foredeep (zone No. 18) is situated in Iraq between the Zagros Fold-Thrust Belt and the stable Arabian Plate (Fig. 9), forming the northeast edge of the Arabian Platform (Onur et al. 2017). It has many concealed geologic structures, which affect the stratigraphy and geomorphology of several recent landforms, reflecting neotectonic activity (Fouad and Sissakian 2011). The thickness of the Quaternary soft sediments in the Mesopotamian region varies from 3 km in the north to about 8 km at Kuwait in the south (Gok et al. 2008), which might have a serious amplifying effect on the ground motion.

The Mountain Front Fault

To the north of the Mesopotamia seismic zone, intermittent segments with diverse directions representing the Mountain Front Fault (zone No. 19) are present (Fig. 10). The Mountain Front Fault is one of the main structures that is responsible for the tectonic subdivisions in the Zagros Fold-Thrust Belt and the strong variations in topography and geologic structures across the belt. This seismic zone is characterized by a higher seismic activity than its southern limits (Fig. 9). Many earthquakes with Mw greater than 5.5 were recorded in this seismic zone, with a maximum recorded event of Mw 6.3. Fault plane solutions of large events depict thrust faulting as a sense of motion.

The Posht-e Kuh Arc

North of the Dezful Embayment seismic source zone, the High Zagros and the Simple Fold Belt are together recognized as the Posht-e Kuh arc (zone No. 21). It is almost parallel to the frontal structures to the NW and SE (Allen and Talebian 2011). Right and left lateral strike-slip faults bound the western side and the eastern side of the arc respectively. It is separated from the High Zagros Thrust Belt, because the extension of Main Zagros Thrust Fault becomes of strike-slip nature in this area (Figs. 6 and 7).

The Kirkuk Embayment

The Kirkuk Embayment (zone No. 22) is a part of the Zagros Fold-Thrust Belt, which is relatively narrow in this area and is lacking for an efficient Hormuz salt detachment. The Kirkuk Embayment contains the northwest-southeast trending

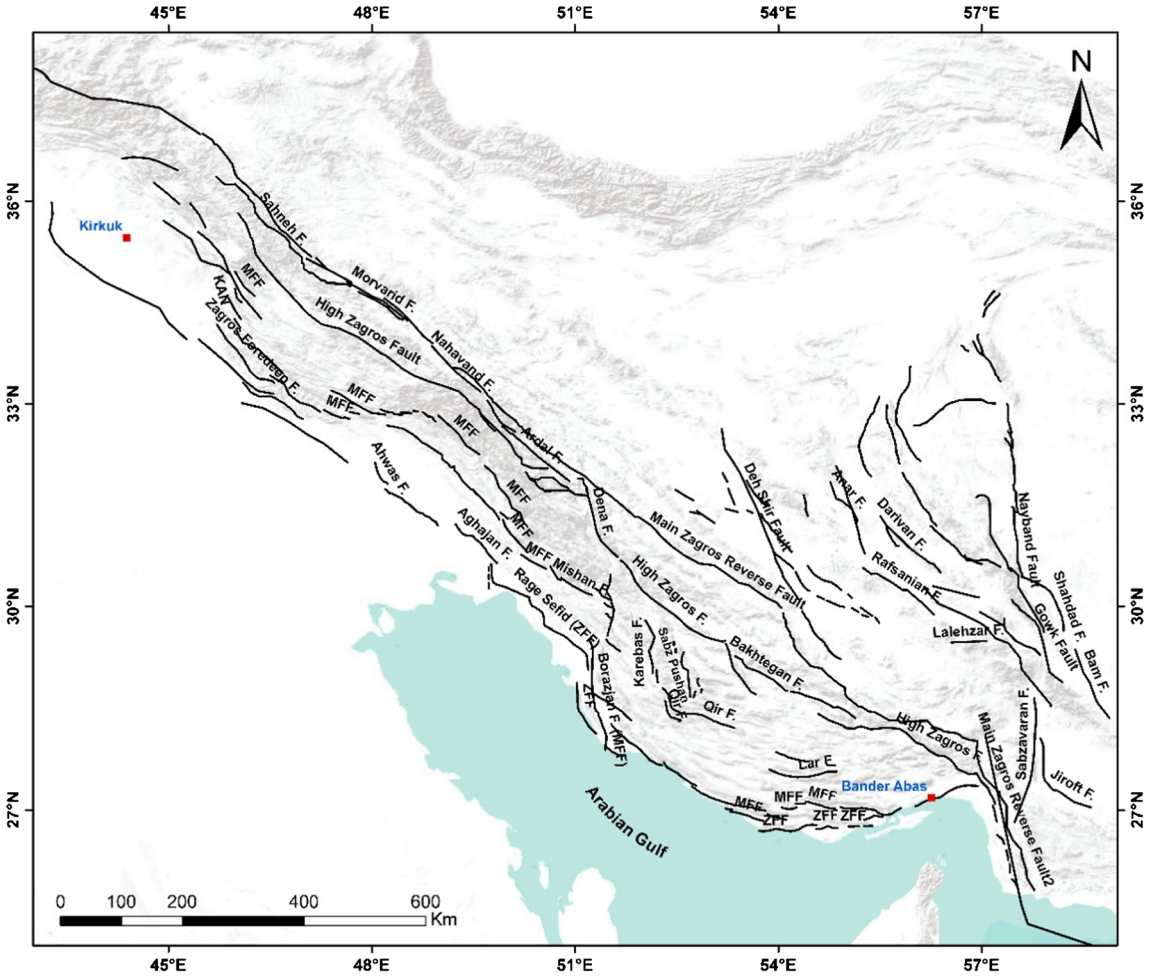

Fig. 10 Active faults of the Zagros Fold-Thrust Belt (modified after Hessami et al. 2003)

anticlinal, the seismically active structures of the ZSFB in northeastern Iraq. It is usually considered as a subdivision of the Zagros Belt (e.g., Authemayou et al. 2005; Alavi 2007). Shortening rate across the various segments of the Zagros Fold-Thrust Belt is found to be at 16–30% in Iran (Alavi 2007), and at 33% in the Kirkuk Embayment (Ibrahim 2009). Therefore, Kirkuk embayment is considered as a separate seismic zone (Fig. 9).

The Zagros strike-slip source zones

Four principal right lateral strike-slip faults are traversing the Zagros folds. These transverse faults are the Kazerun-Borazjan, the Karebas, the Sabz Pushan, and the Khanaqin Faults (Fig. 10). The polygons surrounding these faults are areas within which the reported earthquakes are supposed to be related to these faults. Focal mechanisms of the earthquakes along these faults indicate steeply-dipping strike-slip faults with minor dip-slip movement. Following is a more detailed description of each active strike-slip fault.

The Kazerun-Borazjan Fault The Kazerun-Borazjan is a NS striking active fault. It comprises two right stepping faults (Kazerun and Borazjan) with a gap between them (Berberian 1981). The Kazerun Fault (zone No. 15), about 125 km long, experienced some historical and recent earthquakes with Mw of order 6.0 (Fig. 9). The remnants of Bishapur (the capital of Sassanian) show signs of earthquake impacts of the same size (Berberian 1995). The seismic activity of the Kazerun Fault is verified by the occurrence of historical and instrumentally recorded earthquakes with dextral strike-slip mechanisms on the fault (Baker et al. 1993; Yamini-Fard et al. 2007). The felt region of August 15, 1892 event of Mw 5.6 and that of July 12, 1986 of Mw = 5.5 were located on the Kazerun segment with NS orientation in line with the fault. Paleoseismological studies on Kazerun Fault identified at least two paleo-earthquakes that took place in the last 9 ka, with vertical motion of about 1.5 for each event (Bachmanov et al. 2004). GPS measurements predict slip rate of about 3.6 ± 0.6 mm/year on the Kazerun Fault (Tavakoli et al. 2008).

The 180 km length of the NS Borazjan Fault (zone No. 16) is running to the south of the Kazerun Fault. The Borazjan

shows various signs of recent activity and has a visible scarp at several areas along its strike. Based upon geologic evidences, Bachmanov et al. (2004) estimated a long-term rate of slip of 4–5 mm/year. The centroid moment tensor (CMT) solution of the December 16, 1990 event of Mw = 5.7 reveals NNW-SSE trends, indicating rotation of the basement thrust as a result of the dragging of the Borazjan segment.

The Karebas Fault The Karebas Fault (zone No. 14) of 160 km long is located 65 km to the east of Kazerun Fault (Fig. 10). It crosses through Zagros anticlinal axes and displaced them for at least 10 km (Berberian 1995). No large earthquake is reported to be directly related to the activity of the Karebas Fault (Fig. 9). The maximum observed magnitude on this fault is 4.6.

The Sabz Pushan Fault The Sabz Pushan (zone No. 11), right lateral strike-slip fault, trending NNW-SSE is situated to the east of the Karebas Fault (Fig. 9). This fault zone comprises a distorted en-echelon pattern with offset between the en-echelon segments varies from 5 to 30 km. GPS measurements show slip rate of 1.5 mm/year with an uncertainty of 0.2 mm/year at this fault (Tavakoli et al. 2008). The felt region of the June 25, 1824 earthquake with Mw 6.3 is elongated parallel to the northwestern extension of the Sabz Pushan Transverse Fault (Berberian 1995).

The Khanaqin Fault The NS trending Khanaqin Fault (zone 20) is the eastern boundary of the Kirkuk Embayment, running close to the Iraqi-Iranian borders (Figs. 9 and 10). The NW trending folds of Zagros belt are traversed and displaced along the Khanaqin right lateral strike-slip fault. The Mountain Front Fault is also dislocated right laterally for about 130 km (Hessami et al. 2001). Several earthquakes with magnitude up to 6.1 occurred in this zone. An earthquake swarm with more than 270 seismic events were reported by Iraq Seismic Network (ISN) to occur at Khanaqin and surrounding areas in 2013 with Mw reaching 5.6 (Alridha and Mohammed 2015).

Seismic zones of the transition area between Makran and Zagros

The NNW-striking Zendan-Minab Fault is regarded as a deformed transition zone between the Zagros Collision and the Makran Subduction Zone (Fig. 10). Peyret et al. (2009), using geologic and GPS measurements, indicated that a slip rate of about 15 mm/year in N10° E is accommodated by two fault systems named the Minab-Zendan Fault (zone No. 5) and the Jiroft-Sabzevaran Fault (zone No. 6). GPS studies and geomorphic investigation indicate that the Minab-Zendan fault is moving at a rate ranging from 7 to 10 mm/year (Bachmanov et al.; Regard et al. 2005). The seismicity of these two faults is low compared to that at Zagros and Makran seismic zones (Fig. 8). Most of the earthquake activity in this area is limited to the west of the Jaz Murian Depression along the Jiroft-Sabzevaran Fault, while much less activity seems to be associated with the Zindan Fault.

Moderate to large size events occurred within these fault systems with dominant low-angle thrust and strike-slip sense of motions, in consistence with NS to NE-SW shortening. The epicentral distribution in this area indicates a progressive transition zone in the lower crust rather than a sharp transform fault (Yamini-Fard et al. 2007).

The Aliabad Seismogenic Zone

The Aliabad Seismogenic Zone (zone No. 7) is situated at the bend, where the MZRF changes its NW-SE direction to N-S along the Minab-Zendan (Fig. 8). It is characterized by its high seismicity. The focal mechanism solutions of the earthquakes occurred on March 21, 1977 and March 04, 1999 indicate reverse faulting mechanism with NE-SW direction. This mechanism and related strike direction do not match any of the mapped active faults by Hessami et al. (2003). Thus, this zone is considered as a separate area source.

The Gowk Fault Zone

Although the Gowk Fault (zone No. 8) is not associated with any of the Arabian Plate boundaries, it is considered in the current study due to its potentiality to generate great earthquakes and its proximity to the Arabian Peninsula (Fig. 10). It is a major N-S right lateral strike-slip fault that witnessed a number of moderate to large earthquakes (Fig. 8). Berberian and Yeates (1999) provided that earthquakes of magnitude up to 8.0 can take place on this fault.

The Oman Mountains

The Oman Mountains (zone No. 56) occupy northern Oman (Fig. 7), showing many features for recent tectonic activity (Johnson 1998; Kusky et al. 2005). Some of these features are associated with recent cutting in drainage, faulting, and irrigation systems. Kusky et al. (2005) demonstrated the existence of some tertiary faults with clear dislocations. Evidences of historical seismic activity in the region are also present (Ambraseys et al. 1994; Kusky et al. 2005; Musson 2009). Oman seismic network (OSN) reported many small felt earthquakes in Oman Mountains since 2001. Furthermore, on 11 March, 2002, an earthquake of Mw 5.0 took place within the northern part of Oman Mountains and was felt in northern Oman and UAE (Fig. 8).

The Abdel Aziz-Sinjar area

Abdel Aziz-Sinjar area (zone No. 23) in northeastern part of Syria is an extensional structure related to the locking of the Neo-Tethys. A Neogene compression is observed due to the frequent collisions along the northern Arabian Plate during the period from the Late Cretaceous to the Late Miocene, leading to the inversion and shortening of the Abdel Aziz-Sinjar Graben (Brew 2001). Some contemporaneous NE-striking normal faults have been identified in this high structure zone. Its eastern margin is marked by the northwestern end of the Kirkuk Embayment (Fig.6).

Seismic source zones of eastern Anatolian collision

The North Anatolian and the East Anatolian Fault collectively accommodate the WSW motion of the Anatolian Plate due to the ongoing collision of the Arabian with the Eurasian Plates. Three seismic zones were delineated in this area (Fig. 9): the East Anatolian Fault (zone No. 26), the Bitlis Suture Zone (zone No. 24), and the Karacadag Extension Zone (zone No. 25).

The East Anatolian Fault (EAF) is a left lateral strike-slip fault that limits the northward-moving Arabian Plate to the north. The East Anatolian Fault has a NE trend, starting from the northern end of the Gulf of Aqaba-Dead Sea Fault and extends to meet the North Anatolian Fault. The largest documented events along the East Anatolian Fault occurred in 1114, 1513, and 1893 with Ms. 7.4, 7.4, and 7.1, respectively (Ambraseys and Jackson 1998; Grunthal and Wahlstrom 2012). Only one large earthquake with Ms. 6.5 has been generated on this fault in the twentieth century in 1905. In 2003 and 2010, two earthquakes with Mw 6.4 and 6.1, respectively, hit the East Anatolian Fault in eastern Turkey, killing at least 230 people. Paleoseismological exploratory trenching studies on EAF indicate the rupturing of 1874 and 1875 earthquakes with magnitudes greater than 6.5 and the occurrence of other destructive earthquakes prior to these events.

The Bitlis Suture Zone (Fig. 1) separates the Arabian Plate from the Anatolian Plate. Along this zone, the Arabian Plate collides with the Anatolian Plate indicating NS compression. This seismic source zone experienced earthquakes of order of Mw 6.0, indicating reverse faulting. The largest recorded event in this seismic zone is Leice earthquake of 1975 with Mw 6.4.

The Karacadag extension seismic source zone (zone No. 25) is located on the Arabian Foreland (Fig. 9), including a tectono-stratigraphic succession of mainly shelf sediments that lies unconformably on the basement (Al-Shijbi 2013). The Kurtalan earthquake on March 24, 1964 with Mw 6.0 is related to extensional fissures of Karacadag due to the NS compression of the Arabian Plate.

Seismic sources of the Gulf of Aqaba-Dead Sea Fault

The Gulf of Aqaba-Dead Sea Fault (ADSF) is a seismically active zone with a length of about 1100 km. Most of the seismicity occurs along the geologically recognized borders and margins of this transform system, condensing in the deep areas of the Gulf of Aqaba and the Dead Sea. Both seismicity and GPS measurements indicate the activity and the possibility of occurrence of large earthquakes almost along all segments of this fault. A comprehensive review on the paleoseismological and slip rate studies in the ADSF is provided by Meghraoui (2015).

The Aqaba earthquake on November 22, 1995 with Mw 7.3 is the strongest recorded event in the twentieth century. Paleoseismological and historical studies demonstrate the occurrence of moderate to large earthquakes with Mw > 7 along the ADSF, causing extensive damage to historical structures (e.g., Wetzler et al. 2010; Lazar et al. 2010; Meghraoui 2015). A low to moderate seismic activity is occurring at the intraplate regions, mainly in the north (Fig. 2). The ADSF shows varying trend, structural style, and reported seismic activity. The ADSF changes its strike alternatively from NE-SW to NS giving rise to four main segments, namely the Gulf of Aqaba-Wadi Araba, the Dead Sea Rift, Lebanon Mountains, and the area surrounding Missyaf and Ghab Faults (Fig. 11).

The Gulf of Aqaba-Wadi Araba segment

The internal of the Gulf of Aqaba (zone No. 36) is engaged by three elongated pull-apart, en-echelon basins (Fig. 11) that are controlled by longitudinal strike-slip faults within the gulf (Ben Avraham et al. 1979). Deif et al. (2009a) considered each of these basins as a separate seismic source zone. Such superfluous detailing for the zones may not be required for the current regional study since it may lead to unreliable estimations of recurrence parameters in the upcoming hazard study.

The Gulf of Aqaba occupies the most southern part of the active Aqaba-Dead Sea Fault (Fig. 12). No instrumental information was available on the seismicity along the Gulf of Aqaba-Wadi Araba segment until 1983, when more than 500 events with a maximum Mw of 5.2 were reported in the Gulf of Aqaba. Two more seismic sequences occurred in 1993 and 1995 with maximum Mw 6.1 and 7.3 respectively. The main shock of 1995 sequence was followed by a series of aftershocks activity for about 6 months (Baer et al. 2008). Focal mechanism solutions and stress tensor inversion for large earthquakes show strike-slip mechanisms almost in the NS direction with dominant tension stress (Abdel Rahman et al. 2009). This activity contradicts the earlier apparent aseismic nature of the Gulf of Aqaba, but concurs with the field evidences for recent crustal movement (Garfunkel 1970).

Wadi Araba (zone No. 35) stretches from the Gulf of Aqaba to the southern edge of the Dead Sea for about

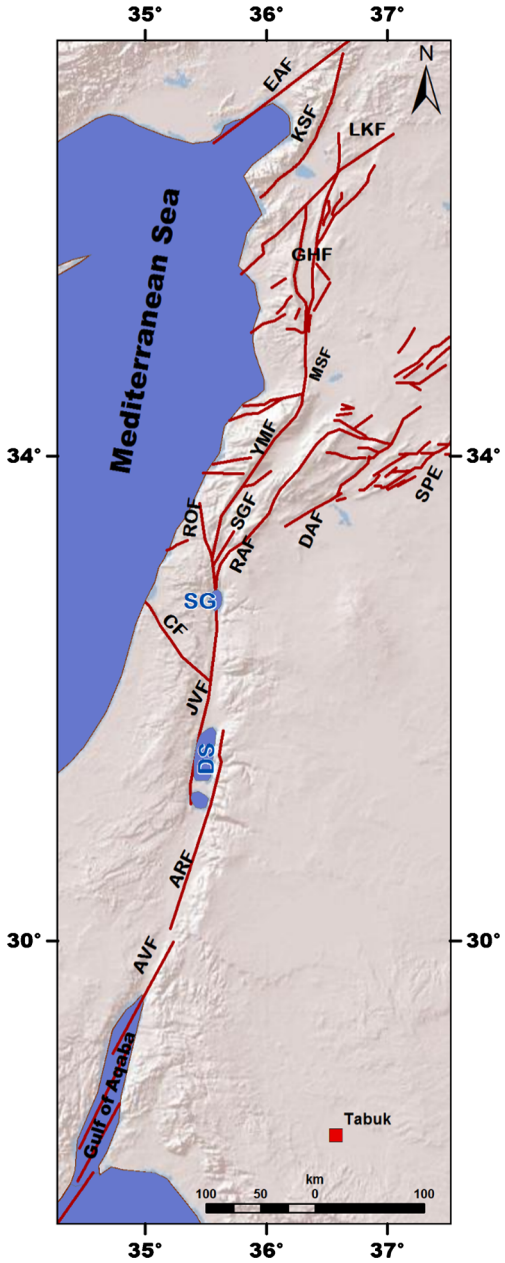

Fig. 11 Main tectonic structures of the Aqaba-Dead Sea Fault, compiled after Gomez et al. (2007) and Asfahani and Darawcheh (2017). Abbreviations for principal faults and areas: *AVF* Avrona Fault, *ARF* Araba Fault, *DS* Dead Sea Fault, *JVF* Jordan Valley Fault, *SG* Sea of Galille, *SPE* Southern Palmyride Fault, *RAF* Rachaiya Fault, *SGF* Serghaya Fault, *CF* Carmel Fari's Fault, *ROF* Roum Fault, *YMF* Yammouneh Fault, *MSF* Misyaf Fault, *GHF* Ghab Fault, *KSF* Kara Su Fault, *LKF* Latakia-Kelles Fault, *EAF* East Anatolian Fault

160 km (Klinger et al. 2000). Faults in this area show evidences for left-lateral strike-slip sense of motion. Although the low seismicity of Wadi Araba compared to its surroundings, four large earthquakes are thought to have occurred in 1068, 1212, 1293, and 1458 with estimated magnitudes a little smaller than that of the 1995 event (Poirier and Taher 1980; Garfunkel et al. 1981; Klinger et al. 2000). Ambraseys et al. (1994) located 1068 earthquake in Tabuk area to the southeast of the Wadi Araba.

No large instrumental or historical earthquakes were reported in the Wadi Araba since 1458. Paleoseismic evidences proves the occurrence of several large earthquakes ($M > 6$) during the Pleistocene and the Holocene in Wadi Araba, and the potentiality of a damaging earthquake in this zone in the future must be utterly considered (Zilberman et al. 2005; Klinger et al. 2015). Fault plane solutions support the pure sinistral strike-slip motion along nearly NS plane for this source. Using cosmogenic radionuclide (CRN) dating of embedded cobbles at one site on the fault, Le Beon et al. (2010) suggested slip rate range of 5.4 ± 2.7 mm/year over the last 11.1 ± 4.3 ka, which seems in coincidence with average slip rate of 4.7 ± 1.3 mm/year since 15 ka calculated by Niemi et al. (2001). Based on a precise GPS velocity field, Masson et al. (2015) obtained a velocity of 4.9 ± 0.5 mm/year. Due to the vast variation in the seismicity level, the Gulf of Aqaba and Wadi Araba were considered as two separate seismic zones (Fig. 12).

The Dead Sea Rift segment

This segment is a basin inter-basin system that extends from the Dead Sea in the south through the Jordan Valley, and further to the north to the Sea of Galilee. It includes two seismic source zones. The first one (zone No. 34) is the Dead Sea Basin (DSB), which is bounded by the Wadi Araba Fault to the east and the Jordan Fault to the west (Fig. 12), which is a major left lateral strike-slip fault en-echelon to the Araba. Therefore, the DSB is characterized by this double-fault system and hence the relatively high seismicity. This part of the segment is considered as a separate seismic source zone (Fig. 12). Stress tensor inversion results show, generally, left lateral strike-slip faults with considerable normal component due to the dominant N37° E tension stress (Abdel Rahman et al. 2009), in accordance with Hofstetter et al. (2007).

The second seismic source (zone No. 31) includes the Jordan Valley and Hula Kineret Basins. The inter-basin of Jordan Valley runs north to south for about 100 km, connecting the DSB in the south to the Sea of Galilee in the north. The edges of the valley are bordered mainly by faults to the east and west (Al-Zoubi et al. 2006). A small amount of local compression close to the Jordan Fault was observed (Garfunkel et al. 1981). Earthquake activity along the Jordan Valley is low compared with the DSB to the south. Therefore, it is separated from the DSB and is considered as a distinct seismic source zone (Fig. 12). This zone experienced relatively strong earthquakes (e.g., 1927 with Mw 6.3). Paleoseismic studies prove the activity of this segment which hosted (at least partly) the 702, 1202, and 1759 earthquakes (Gomez et al. 2003; Marco et al. 2005; Daeron et al. 2007; Nemer et al.

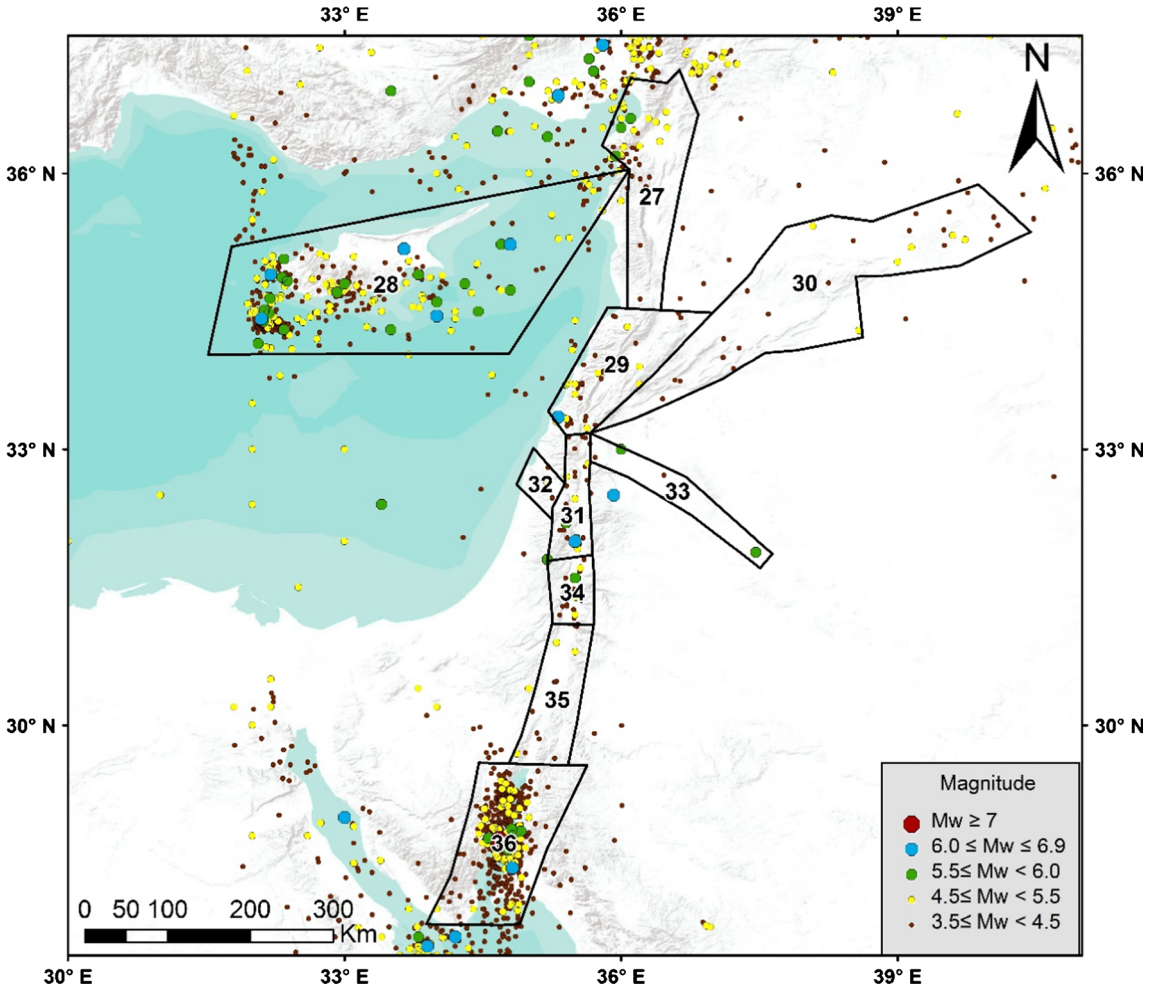

Fig. 12 Detailed seismic source zones and seismicity of the Gulf of Aqaba-Dead Sea Fault

2008; Ferry et al. 2011). Moreover, Ferry et al. (2011) identified 12 seismic ruptures in the Jordan Valley during the last 14 ka. Stress tensor inversion for nine focal mechanisms (Abdel Rahaman et al. 2009; Palano et al. 2013) indicates a dominant NE tension stress. The NNW trend is the preferred ones for rupturing along this zone. Results of paleoseismic and the archaeo-seismology along with the historical seismic record indicate an average slip rate of 5 mm/year over the last 25 ka (Ferry et al. 2011). North of the Jordan Valley, the Hula and Kineret pull-apart basins (HKB) are present. Seismic activity in the HKB has been recorded up to the bend of the transform at the beginning of the northeast trending Lebanon Mountains.

Lebanon Mountains segment

This segment (zone No. 29) starts where the rift switches its direction to the northeast, resulting in the transverse compressional zone of the Lebanon Mountains. Sykes and Seeber (1982) described these bends as tectonic knots forming areas of significant stress buildup. Yammuneh is the main fault of the ADSF, accommodating most of the plate motions (Marco and Klinger 2014). However, Roum, Rachaya, and Serghaya active faults, which splay to the west and east from the Yammuneh Fault may be seismically important. The seismicity within this bend is scattered so that the seismogenic belt is wide, on contrary to the south, where the seismic zones are relatively narrow. So, it is difficult to attribute the reported seismicity to any of the known faults. Thus, this bend is considered as one seismic source zone (Fig. 12). Daeron et al. (2004) calculated slip rate of 5.1 ± 1.3 mm/year during the late Pleistocene–Holocene for Yammouneh Fault from alluvial fan offsets by the fault. Slip rates along other faults in this segment does not exceed 1.5 mm/year (Nemer and Meghraoui 2006; Nemer et al. 2008). Paleoseismic investigations indicate the activity of this segment on which the earthquakes of 1202 and 1759 are bracketed with the Jordan Valley Fault (Gomez et al. 2003; Marco et al. 2005; Daeron et al. 2007; Nemer et al. 2008). Daeron et al. (2007) shows a sequence of 10–13 coseismic evidences in the last 12 ka along Yammouneh segment. Stress tensor inversion (Palano et al. 2013) indicates a dominant normal faulting.

The Ghab Basin

The northern part of the ADSF is dominated by the NS Missyaf and Ghab Faults (zone No. 27). GPS measurements (Gomez et al. 2007 and Alchalabi et al. 2010) show variable slip rate along the Lebanon Mountains bend and the Ghab Basin area, which may indicate a complex transform. This seismic zone shows variation of slip rate from 7.5 mm/year at the contact with EAF to about 1.8 mm/year at the southern edge of the Ghab Valley (Palano et al. 2013). Although its apparent quiescence since the beginning of the twentieth century, Alchalabi et al. (2010) show evidences of recent shearing along this segment. This area is distinguished from the Lebanon Bend Zone due to its different trend and slip rate (Fig. 12). Akyuz et al. (2006) provided geological evidences on the occurrence of 859, 1408, and 1872 historical earthquakes. Using stress tensor inversion technique, Palano et al. (2013) show a dominant normal faulting regime.

Seismic sources branch of main ADSF

Although the ADSF is the major source of earthquake generation in the transform area, three main seismic sources are branching from it, namely the Carmel Fari'a Fault, the Wadi Sirhan Graben, and the Palmyride.

The Carmel Fari'a active fault The Carmel Fari'a Fault (zone No. 32) is a seismically active structure with a left lateral strike-slip movement that runs northwest from the Jordan Valley to the Mediterranean Sea with uncertain termination (Fig. 12). Several GPS measurements along the Carmel Fault shows an oblique motion with comparable left-lateral 0.7 mm/year and NS extension 0.6 mm/year, respectively (Sadeh et al. 2012). Stress tensor inversion and well-constrained focal mechanisms depict a dominant tension with a preferred rupture plane along NW (Abdel Rahman et al. 2009).

The Sirhan Fault Wadi Sirhan Graben (zone No. 33) is the most important secondary geologic structure in Jordan (Fig. 12). It includes complex sets of NW-SE and EW-oriented normal and strike-slip faults (Kazmin 2002). It extends for about 325 km from the Kingdom of Saudi Arabia to northern Jordan. WSG is terminated at its northwestern border by the ADSF at the Hula and Kineret Basin. This fault series was initiated by transitional forces generated during the evolution of the Red Sea (Ramşay 1986; Camp 1984). This fault is considered in the current study because some earthquakes of order of Mw 5.0 occurred along it.

The Palmyride Fold-Thrust Belt The Palmyride Fold-Thrust Belt (zone No. 30) extends NE across central Syria and comprises several asymmetrical anticlines, which are separated by narrow depressions (Figs. 11 and 12). Brew et al. (2001) stated that this belt is created as a result of regional compressional stress due to the opening of the Neo-Tethys as well as the eastern Mediterranean. The Palmyrides has been influenced by intermittent compression since the Late Cretaceous resulting in folding and the present topographic uplift. Ben Menhem (1979) located a historical destructive earthquake of ML 7.2 in 1042 in the Palmyride area. More recent studies do not include this event (e.g., Ambraseys et al. 1994; Grunthal and Wahlstrom 2012). If the location of this event is accurate, the consequences on the seismic hazard assessment will be huge.

The Cyprus seismic source

The Cyprus (zone No. 28) lies within the Alpine-Himalayan belt, which contains about 15% of the global seismicity. The seismicity of Cyprus is due to the presence of the Cyprus Arc at which the African and the Anatolian Plates meet, forming a subduction zone that slips at 18 mm/year. Earthquakes are concentrated in the south and west parts of the island (Fig. 12). Several historical and instrumental earthquakes with Mw greater than 6.5 occurred mainly to the south of Cyprus (e.g., the earthquakes of 342, 1222, and 1996). This seismic zone is characterized by the occurrence of intermediate depth earthquakes at the central part of the Cyprus Arc. Generally, the earthquake activity along the Cyprus Arc is relatively less than that of adjacent Aqaba-Dead Sea Fault and East Anatolian Fault.

Seismic zones of the Arabian Shield and the Red Sea

The Arabian Shield is an ancient, trapezoidal shape land mass (Fig. 13). The formations and structures associated with the Arabian Shield are properly reviewed by Johnson et al. (2011), and Johnson and Kattan (2012). The Arabian Shield consists mainly of metamorphic rocks surrounded by the Phanerozoic deposits. It is separated from the Red Sea by a narrow Cenozoic coastal plain (Johnson and Woldehaimanot 2003). The Phanerozoic deposits comprise younger sedimentary rocks with thickness reaching 10 km (Bosence et al. 1996). Since the Oligocene, the western and southern boundaries of Arabia were uplifted and partially covered by basalt, leading to the formation of the Harrat (volcanic fields) and the Red Sea escarpment.

Al-Amri et al. (2004) showed that several tectonic terranes were created due to the formation of the Arabian Plate through an accretion process. These terranes are separated by major suture zones or by NW trending faults (Fig. 13). Each terrain has specific stratigraphy, structure, and geochemical features that distinguish it from adjoining terrane. The western part of the Arabian Shield is composed of the Midyan terrane, Hijaz terrane, Jeddah terrane, and Asir terrane from north to south (Fig. 13). The eastern part comprises Arryan and Afif terranes,

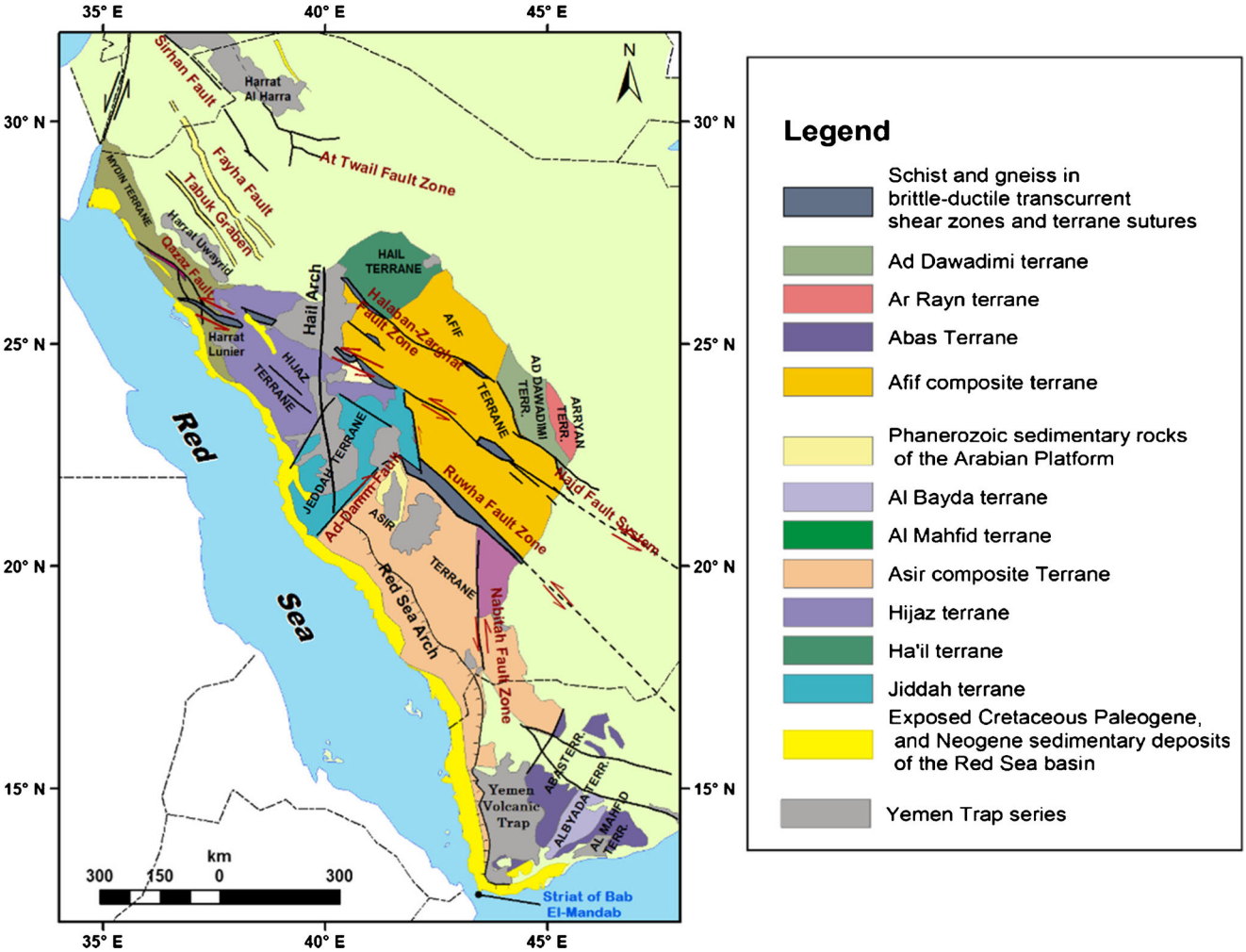

Fig. 13 Main geologic structural elements of the Arabian Shield. Modified after Johnson (1998), Bosworth et al. (2005), and Al-farajat et al. (2016)

which is separated from the western terranes by the prominent Najd Fault System.

The Red Sea is a rare tectonic, warm water body at which the development of the oceanic accretion by means of continental rifting can be realized. It is a NW-SE trending, elongated young oceanic zone of some 2000 km long and a maximum width of about 350 km. The Red Sea connects with the Gulf of Aden via the Strait of Bab El-Mandab, where the Red Sea has a minimum width of about 30 km. The seafloor spreading and thus oceanic crust is well recognized up to 20° N. This process of active oceanic spreading controls the increasing drift of the Arabian Plate. The oceanic crust is not outcropped in the northern Red Sea.

Seismic activity is most pronounced along the rift axis of the Red Sea, where more than 83% of the seismic moment is released (El-Isa 2015). The most southern area of the Res Sea between the mouth of the Gulf of Aden and latitude 20° N shows prominent seismic activity (Fig. 2). A lower level of seismicity takes place within the Arabian Plate away from the spreading center. Inland earthquakes are clustered in Yemen volcanic trap, Jizan, along the Ad-Damm Fault in Jeddah Terrane, Al-Madinah and its adjacent area, and Tabuk area. The seismicity of Red Sea decreases northward till Sinai triple junction where the Red Sea faults meet the NW-SE Gulf of Suez and the NE-SW Gulf of Aqaba faults, indicating that the middle part of the Red Sea is of lower seismic activity compared with the most southern and northern parts (El-Isa 2015). The seismicity at this junction is relatively high.

Many locations in the western part of the Arabian Plate are volcanically active and associated with moderate earthquake activity. The volcanic activities are distributed mainly along the NS trending, Cenozoic age Hail Arch Volcanic Line (Fig. 13). Earthquakes of 1122, 1256, and the well-known earthquake sequence that occurred in 2009 are associated with the volcanic activity around Al-Madinah.

The variation between the Arabian Shield and the Red Sea in geologic composition, structures, nature of the crust, and the seismic activity necessitates the separation of the Arabian Shield seismic sources from the Red Sea ones. The contact between the Red Sea basin and Arabian Shield is identified

where the continental crust of the Arabian Plate thins from 40 to 45 km thickness (inland) to 5–15 km (Mooney et al. 1985) near the coast.

During the rifting and sea floor spreading processes, a system of transform and normal faults is formed across and along the Red Sea. Some authors supposed that these transform faults (e.g., Ad-Damm Fault) are extending inland for hundreds of kilometers (e.g., Ambraseys 1983; El-Isa and Al Shanti 1989). Roobol and Stewart (2009) proved that these inland faults are of Precambrian age, which may be reactivated during the Cenozoic due to the opening of the Red Sea. Therefore, the Cenozoic transform faults of the Red Sea, which offset the spreading axis, did not come ashore ones. This supports the idea of separating the shield seismogenic zones from the Red Sea ones.

Shield seismic source zones

The Arabian Shield exhibits different seismicity levels along its western part. Additionally, it shows a dramatic change in the strike of the surface lineaments (Fig. 14). The lineaments vary from almost N-S at Assir Terrain at the south to NE-SW close to Jiddah Terrain at the middle, and become NW-SE at the northwestern part of the shield, reflecting the change of stress direction during the formation time of these tectonic terrains (Deif et al. 2009b). The variations in the seismicity, lineament trend, and the surface geology at each terrain are used to divide the Arabian Shield into six distinct seismogenic area sources.

The Yemen seismic source zone The Yemen (zone 42) has been influenced occasionally by earthquakes along the Red Sea and its coastal zone, in addition to inland. The earthquake of Ma'rib Dam that occurred in 460 AC is the oldest recognized devastating event in this zone (Ambraseys et al. 1994). The Dhamar event, 1982 with Mw 6.2, which caused a wide damage, fatalities, and land deformation, took place in a recent volcanic region. It is followed by a relatively high level of aftershocks that extended for about 1 month.

This seismic zone is delineated to model the seismicity of the volcanic trap series (Figs. 13 and 15). The western and southern limits of this zone coincide with the boundaries among the continental crust of Yemen and the oceanic crust of the Red Sea and the Gulf of Aden, respectively.

The Jizan Seismic Source Zone The southern boundary of the Jizan Seismic Source Zone (zone No. 41) separates the Yemen volcanic trap series from the Arabian shield. It is separated from its adjacent northern seismogenic zone due to its relatively high seismicity (Fig. 15). The seismicity within this zone is associated with the Oligocene-Miocene rifting activities of the Red Sea and the volcanic activity. The largest known earthquake occurred here is of 11 January, 1941 with Mw 6.2. On 23 January, 2014, a seismic sequence with the largest earthquake of ML 5.1 hit this seismic zone (El-Hadidy 2015).

The Tihama seismic source zone This seismic zone (zone No. 40) lies to the north of Jizan Seismic Source Zone (JZN) and occupies the majority of Asir geologic terrane (Fig. 15). It is characterized by N and NE trending lineaments (Fig. 14) with complex patterns of strike-slip, normal, and reverse faulting (Greenwood et al. 1980). Ad-Damm Fault indicates the northern boundary of the Tihama Seismic Source Zone (THM) (Fig. 10).

The Jeddah seismic source zone This seismic source (zone No. 39) is distinguished from THM due to its NE trending surface lineaments parallel to the transform faults of the Red Sea (Figs. 14 and 15). Ad-Damm Fault is the most prominent seismological feature of this northeast trending structure and extends from the coastal plain to beyond Al-Taif. Pallister (1984) has inferred Precambrian right lateral movement on this fault. Evidences supporting the activity of this fault come from the micro-earthquake studies carried out by Merghelani (1981) and from the micro-earthquake records of the Saudi National Seismic Network (SNSN). Several historical earthquakes of magnitude of order 5.0 are associated with this fault.

The Hijaz seismic source zone The Hijaz Zone (zone No. 38) takes up most of the Hijaz terrane, where surface lineaments strike mostly NW-SE parallel to the Red Sea axis (Fig. 14). This zone experienced both historical and recent earthquakes. The seismic activity of this zone (e.g., 1256, 1293, and 2009) is clearly associated with volcanic activity. The sequence of 2009 is associated with the volcanic activity in Harrat Lunier. It is relatively well studied and precisely located due to the existence of the enhanced Saudi seismological network, which is operated by the Saudi Geological Survey (SGS). The sequence of 1256 looks larger than 2009 sequence, with prominent volcanic eruption extended for 3 months. The exact location of 1256 crater is unknown, but many earthquakes were felt in Al-Madinah, causing the collapse of a number of houses. The1293 sequence was associated with a minor volcanic eruption Near Al-Madinah.

The Tabuk seismic source zone This zone (zone No. 37) is characterized by moderate seismic activity concentrated mostly, along Qazaz Fault, along the Red Sea coast, and along the northwest extension of the Najd Fault System at Fayha Fault and Tabuk graben (Figs. 13 and 15). Tabuk Zone experienced the largest earthquake in the western part of the Arabian Peninsula that occurred to the north of Tabuk on March 18, 1068 with Mw of 7.4. Another damaging earthquake occurred along the extension of Tabuk graben on January 04, 1588 with Mw 7.1 and caused few damages between north Aqaba and Tabuk, Sinai, and Cairo (Ambraseys et al. 1994). In June 2004, a seismic sequence took place at the eastern edge of

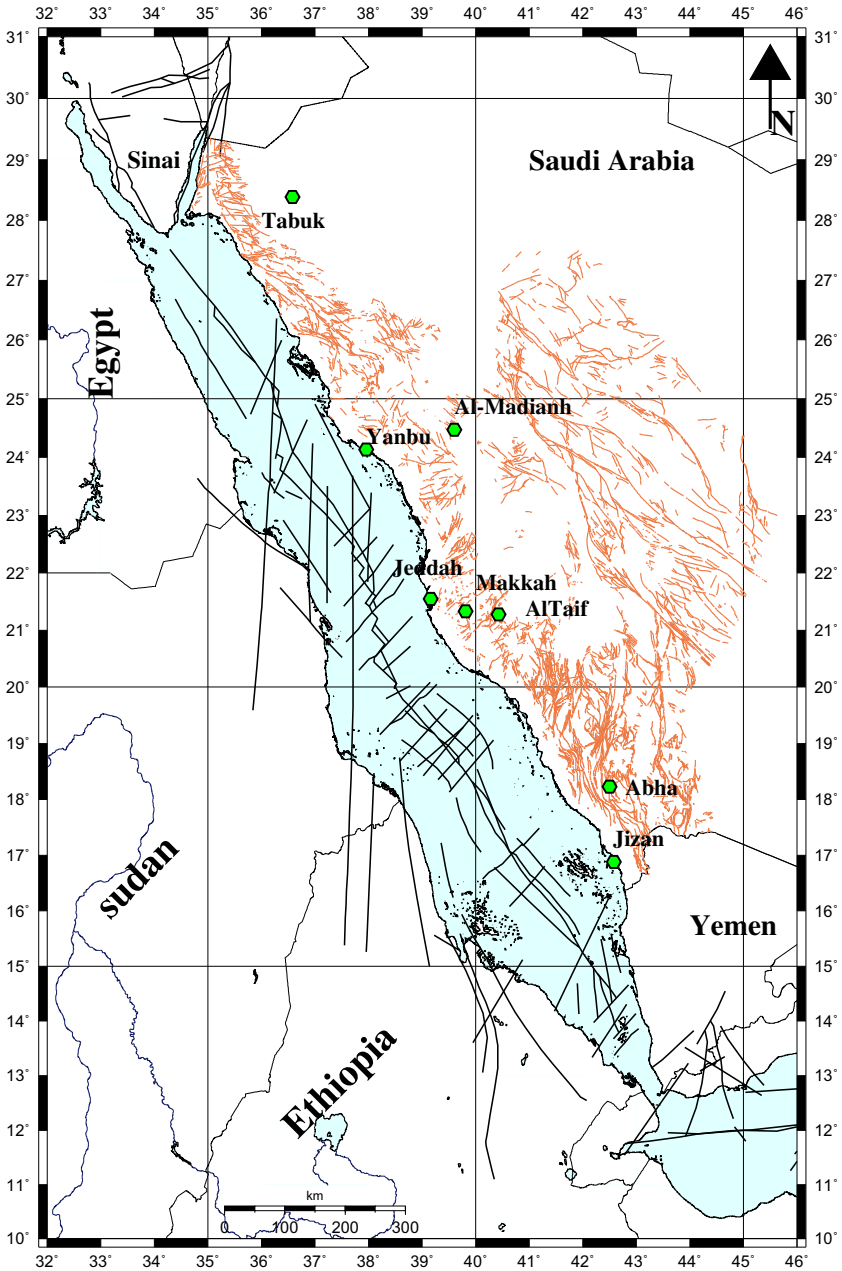

Fig. 14 Surface faulting of the Red Sea and the Arabian shield (after Deif et al. 2009b)

Harrat Uwayrid. At the time of occurrence of this sequence, it is not known whether this cluster is associated with the NW structure in the area or related to the volcanic activity of Harrat Uwayrid (Fig. 13). Xu et al. 2015 used InSAR data to improve the location and source parameters of the largest event of the sequence (Mw 5.1). They found that the main shock activated a normal southwest-dipping fault parallel to the Red Sea rift, at about 70 km southeast of Tabuk City.

The Red Sea seismic source zones

In the current study, the Red Sea is subdivided into six seismic zones. The subdivision is made based on the change in seismicity, occurrence of transverse structures, exposure of oceanic crust on the sea floor, and change in the fault trend along the axial rift.

The Southern Red Sea Zone

This seismic zone (zone No. 43) is very close to the Afar triple junction and has a relatively high seismicity level. The spatial distribution of the epicenters reveals the coincidence between the earthquake locations and the faults along the axial trough and the NE trending transform faults. The seismic activity is distributed all over the seismic zone between the latitudes 12° N and 16.5° N

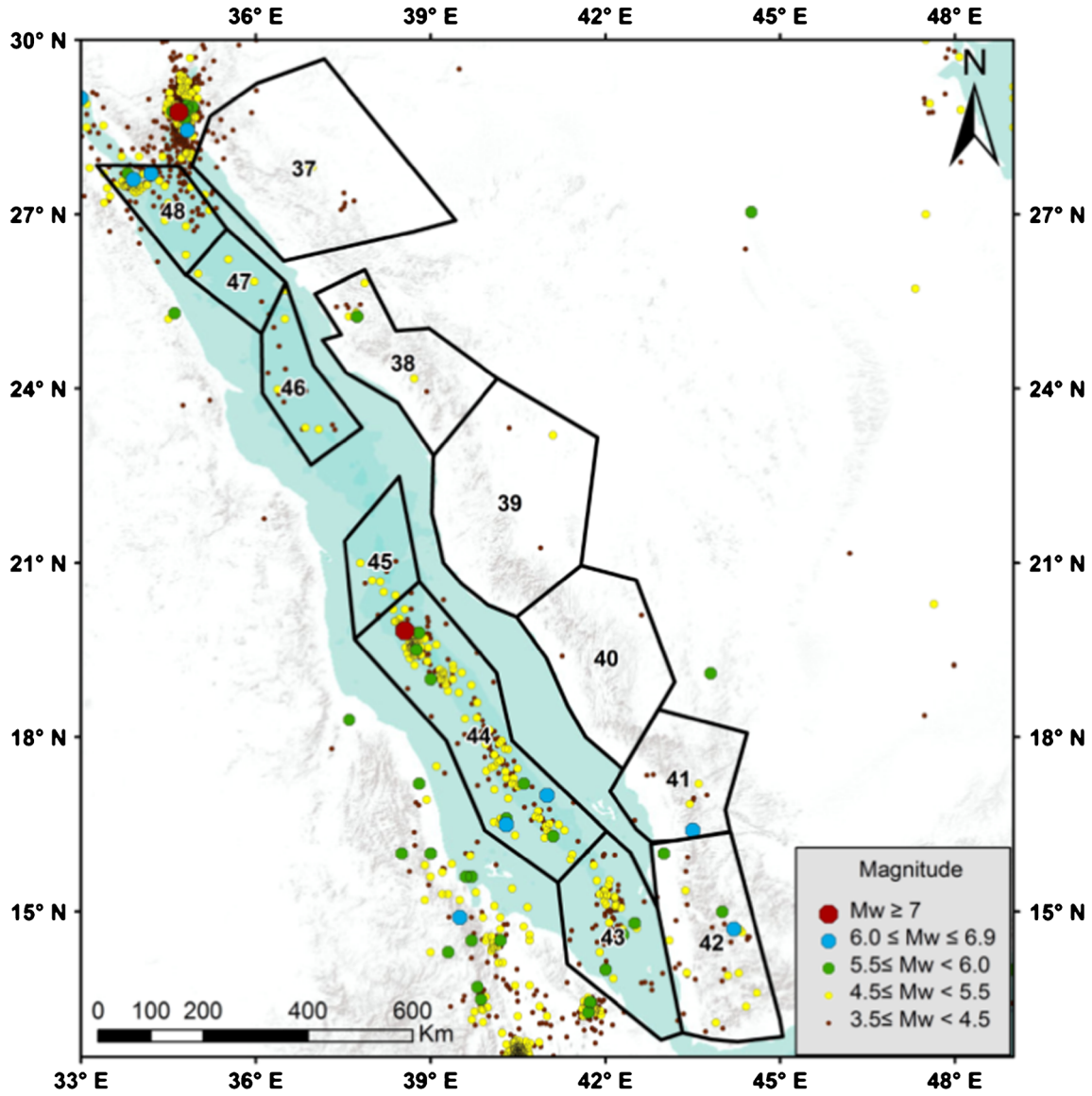

Fig. 15 Seismic source zones and seismicity of the Red Sea and Arabian shield

(Fig. 15). The northern limit of Southern Red Sea (SRS) zone is featured by a clear NE transform fault. The spatial distribution of the epicenters reveals the coincidence between the earthquake location and the faults along the axial trough and the NE trending transform faults, indicating the activity of the two fault systems.

The Central Red Sea Zone

The Central Red Sea Seismic Source (zone No. 44) is characterized by a well-developed axial trough that formed as a result of the seafloor spreading in the last 5 Ma (Girdler and styles 1974). The seismicity is concentrated along the axial trough (Fig. 15). The northern boundary of this zone coincides with the start of the transition zone that separates the oceanic crust in the south from the continental crust to the north. This zone has been hit by a strong earthquake with mb 6.7 in 1967.

The Transition Red Sea Zone

Tectonically, this zone (zone No. 45) is characterized by a discontinuous axial trough that consists of a series of deeps and shallow inter trough zones (Girdler and styles 1974). Faults in this zone are trending almost N-S (Fig. 14). The boundary between Central Red Sea (CRS) and Transition Red Sea (TRS) zones is identified by a significant decrease of seismicity north of latitude 21° N (Fig. 15). No earthquakes were observed between latitudes 22° and 23° N, where the oceanic crust is too thin and hot to produce large earthquakes (Zahran et al. 2016). Thus, no seismic source zones were selected in this range.

The Northern Transition Red Sea Zone

This zone (zone No. 46) is different from TRS that the faults of this zone have NW-SE trend rather than NS in TRS (Fig. 14). The northern boundary at about 25° N coincides with the NE trending transform faults and the associated seismicity (Fig. 15). In this zone, the degree of seismicity is relatively low and scattered compared to the central and southern zones.

The Northern Red Sea Zone

This seismic source zone (zone No. 47) is situated to the north of latitude 25° N, consisting of a broad trough with lacking of a spreading center (Cochran et al. 1986). Recent recorded seismicity may indicate the expected location of the axial rift (Fig. 15). The seismic activity in this zone is much less than the seismicity of Sinai triple junction to the north.

The Sinai Triple Junction Zone

This seismic source zone (zone No. 48) of relatively higher seismic activity (Fig. 15) is characterized by the intersection of three main fault systems, namely the Gulf of Aqaba, the Gulf of Suez, and the Red Sea axial trough faults. Micro-earthquake studies (Daggett et al. 1986) and the seismic observations of National Research Institute of Astronomy and Geophysics (NRIAG), Egypt, indicate that the high seismic activity of the most northern Red Sea does not extend with a similar rate along the entire length of the Gulf of Suez. The focal mechanisms of the large recorded earthquakes in this zone with Mw 6.9 in 1969 and that of 1972 with Mw 5.6 show rather a normal faulting parallel to the Gulf of Suez with strike-slip component (Jackson et al. 1988).

Seismic source zones of Gulf of Aden

The Gulf of Aden is formed due to the movement of the Arabian Plate away from the African Plate. Coleman (1993) showed that most of the sea floor of the Gulf of Aden is oceanic crust. The main feature along the Gulf of Aden is the Sheba ridge spreading center. It extends to the Djibouti, coming close to the Afar triple junction, which composes the Sheba ridge, the Red Sea Rift, and the east Africa continental rift. Sheba ridge is characterized by linear NE trending transform faults, most prominent of them is Alula Fartak, which displaced Sheba Ridge for about 160 km (Fig. 16).

The seismicity of the Gulf of Aden is concentrated along its central axis while some earthquakes occur to the northeast of the Gulf of Aden. These events may be resulted from block adjustments of the motion at the boundary between the African and the Arabian Plates (El-Hussain et al. 2012). The largest observed earthquake at the Gulf of Aden is Mw 6.6 in 2006. The earthquake focal mechanisms along the Gulf of Aden suggest principally a tensile stress. Three main seismogenic source zones were delineated, the Western Gulf of Aden (zone No. 49), the Alula Fartaq Transform Fault (zone No. 50), and the Eastern Gulf of Aden (zone No. 51). A fourth seismic source zone (zone No. 52) is delineated to model the lower seismicity level toward the northeastern part of the Gulf of Aden.

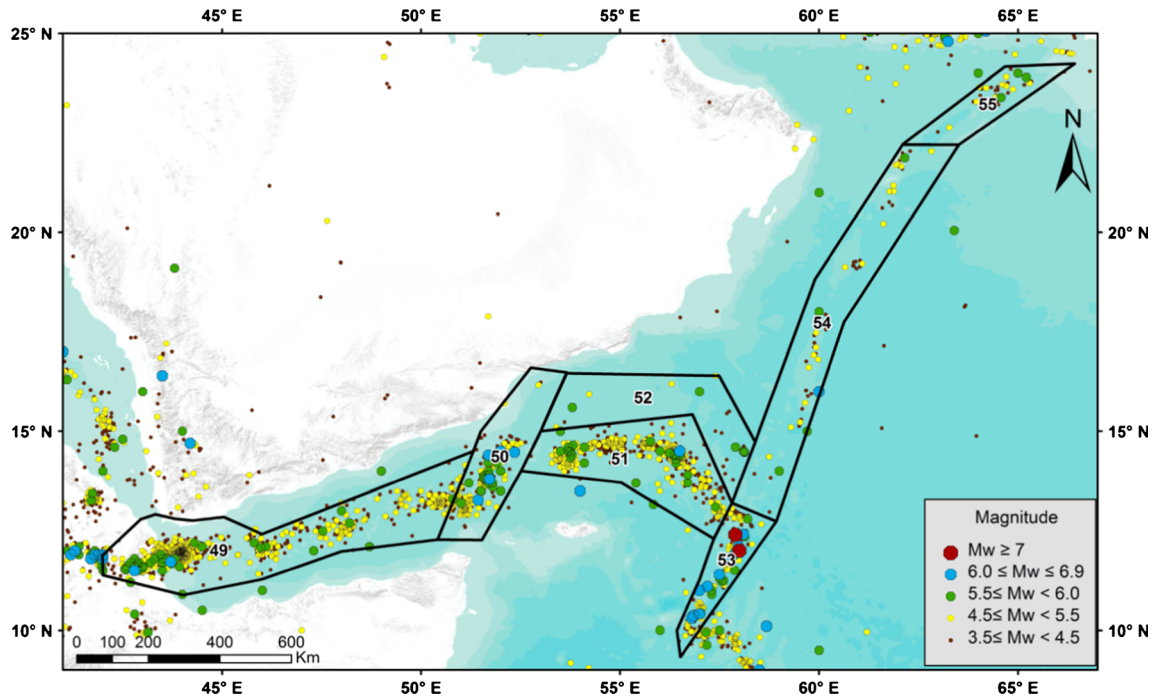

Fig. 16 Seismic source zones and seismicity of the Gulf of Aden and the Owen Fracture Zone

Seismic source zones of the Owen fracture zone

The seismicity along Owen Fracture Zone is low due to the very low relative motion between the Arabian and the Indian Plates. This structure changes its strike to NE-SW in coincidence with the Murray Ridge, which is essentially the continuation of the Owen Fracture Zone to the north. The largest recorded event at the most southern part of Owen Fracture Zone is 7.1, separated from the main structure by Sheba Ridge (Fig. 1). The maximum observed earthquake between Sheba Ridge and Murray Ridge reaches Mw 6.6. Modern earthquakes (as no historical earthquakes are available) on Murray Ridge are smaller than Mw 6.0. Earthquakes along these plate boundaries are characterized by their shallow focal depths. Based upon the seismicity and change in strike, the Owen Fracture Zone is subdivided into three separate source zones (zones No. 53, 54, and 55) to reflect these differences (Fig. 16).

The seismic background zone

A background seismic zone (Zone No. 57) is delineated to join areas with relatively low seismicity levels inside the Arabian Plate (Fig. 6). It extends to include mostly the parts of the Arabian Peninsula that are not included by the delineated seismic sources.

Earthquake recurrence parameters

For any PSHA study, Earthquake catalogs together with the geology and seismotectonic setting of the study area are fundamental in delineating seismic source models and the recurrence parameters that describe the frequency and severity of earthquakes in each seismic source. The earthquake catalog compiled by Deif et al. (2017) is used in this study to determine the recurrence parameters. Such catalog is homogenized in term of moment magnitude (Mw), declustered, and checked for completeness with time.

Seismogenic zones were assumed to generate earthquakes according to a doubly-bounded exponential model (Cornell and Vanmarcke 1969). Therefore, the following truncated exponential recurrence relation is used in the current study to evaluate earthquake recurrency.

$$N(\geq M) = \alpha \frac{\exp[-\beta(M-M\min)]-\exp[-\beta(M\max-M\min)]}{1-\exp[-\beta(M\max-M\min)]} \quad (1)$$

Where $\alpha = N(M_{\min})$, $M_{\min}$ is an arbitrary reference lower magnitude that might affect engineered structures; $M_{\max}$ is the largest earthquake to be generated by seismic source, and $\beta = b \cdot \ln 10$, where b is the slop of Gutenberg and Richter (1956) model.

As the used earthquake catalog (Deif et al. 2017) shows different earthquake completeness levels, coefficients of (Cornell and Vanmarcke 1969) model cannot determined rightly using a direct regression. For that reason, procedure proposed by Kijko and Sellevoll (1992), which consider various times of completeness for different magnitude levels, were used to calculate the coefficients of the used recurrence relationship for each defined seismic source in addition to the regional tectonic area that covers smaller seismic sources (All Makran, All Zagros, Zagros strike-slip faults, All East Anatolian Fault, All Gulf of Aqaba-Dead Sea Fault, All Red Sea, All Aden, and All Owen). Software based theoretically on the Kijko (2004), Kijko and Singh (2011), and Vermeulen and Kijko (2017) is utilized for maximum magnitude calculations. The recurrence parameters and their uncertainties are listed in Table 1.

Discussion and conclusions

The Arabian Peninsula is characterized by rapid growth of infrastructure, leading to a critical need for understanding the seismic activity, the tectonic regime, and the earthquake seismic sources to improve the seismic hazard assessment in the region. Although the interior of the Arabian Plate seems to be stable, its boundaries are responsible for most of the expected seismic hazards. As the data of seismicity, seismotectonic analysis of effective historical earthquakes, and active faulting in and around the Arabian Plate get better, they highly contribute to reduce unknown capable faults and the uncertainties in the association of historical earthquakes with known active faults.

For a reliable seismic hazard assessment, it is crucial to identify, as accurate as possible, the seismic source model that define the geologic structures of potential to initiate seismic activities in the Arabian Plate. An updated homogenous catalog, fault plane solutions, active faults data, tectonic setting, as well as available geological and geophysical data were used to propose 57 seismic source zones. The current model is based upon the most recent available datasets, so that the seismic zones provide a reliable representation on the earthquake occurrence in the region. Some of the used databases were not existed before 2017 (e.g., seismic catalog).

Various seismic source models were proposed for different parts of the Arabian Plate (e.g., Al-Haddad et al. 1994; Tavakoli and Ashtiany 1999; Abdalla and Al-Homoud 2004; El-Hefnawy et al. 2006; El-Hussain et al. 2012; Al-Arifi et al. 2013; Babiker et al. 2015; Zahran et al. 2016). The obtained seismic source model of the current study consists of 57 area source zones. It shows significant variations from the earlier models. Although there is no room to discuss in detail all the differences between the current model and all the previous ones and to give reasons why it differs from them, we will only show some examples of these variations.

Table 1 Earthquake recurrence parameters for the delineated seismic sources. Italic font are the recurrence parameters for the regional tectonic units that contains the delineated seismic sources (All Makran, All Zagros, All Gulf of Aqaba-Dead Sea Fault, All Red Sea, All Aden, and All Owen)

Zone No.	Zone Name	M_{max}	σ M_{max}	M_{min}	M_{max}obs	β	σβ	b	σb	λ	σ(λ)	a
	All Makran	*8.4*	*0.27*	*4*	*8.1*	*1.67*	*0.07*	*0.73*	*0.03*	*6.295*	*0.832*	*3.72*
Zone 1	Makran East	8.4	0.1	4	8.1	1.57	0.14	0.68	0.06	1.822	0.371	2.98
Zone 2	Makran Intraplate	7.8	0.3	4	7.3	1.49	0.16	0.65	0.06	0.860	0.198	2.53
Zone 3	Makran West	6.2	0.23	4	5.9	1.65	0.19	0.72	0.08	0.680	0.167	2.71
Zone 4	Jaz Murian	6.8	0.82	4	6.1	1.56	0.2	0.68	0.09	0.423	0.131	2.35
Zone 5	Zendan Fault	6.3	0.22	4	6.1	1.30	0.2	0.57	0.09	0.465	0.133	1.95
Zone 6	Jiroft Fault	6.0	0.14	4	5.8	1.70	0.17	0.74	0.07	1.268	0.271	3.06
Zone 7	Ali Abad	6.8	0.18	4	6.6	1.52	0.14	0.66	0.06	2.157	0.411	2.97
Zone 8	Gowk Fault	7.5	0.34	4	7.2	1.68	0.13	0.73	0.06	1.602	0.299	3.12
	All Zagros	*7.5*	*0.12*	*4*	*7.4*	*1.84*	*0.04*	*0.8*	*0.02*	*21.625*	*2.165*	*4.53*
Zone 9	Arabian Gulf	6.2	0.26	4	6.1	1.74	0.16	0.76	0.07	1.821	0.368	3.30
Zone 10	Zagros Foredeep	6.8	0.21	4	6.7	1.83	0.11	0.79	0.05	3.359	0.52	3.69
Zone 11	Zagros Simple Fold	6.9	0.21	4	6.8	1.82	0.07	0.79	0.03	8.820	1.16	4.11
Zone 12	High Zagros	7.6	0.24	4	7.4	1.75	0.1	0.76	0.04	3.094	0.468	3.53
Zone 13	Sabz Pushan Fault	6.3	0.34	4	6.1	1.69	0.19	0.73	0.08	0.686	0.184	2.76
Zone 14	Karebas Fault	5.8	0.46	4	5.4	1.81	0.22	0.78	0.09	0.314	0.104	2.62
Zone 15	Kazerun Fault	6.0	0.21	4	5.9	1.60	0.19	0.69	0.08	1.621	0.417	2.97
Zone 16	Borazgan Fault	5.8	0.22	4	5.7	1.61	0.19	0.7	0.08	0.989	0.281	2.80
Zone 17	Dezful Embayment	6.8	0.12	4	6.7	1.86	0.1	0.81	0.04	5.340	0.817	3.97
Zone 18	Mesopotamia	6.5	0.3	4	6.4	2.15	0.18	0.93	0.08	1.670	0.263	3.94
Zone 19	MFF	6.4	0.22	4	6.3	1.59	0.15	0.69	0.06	1.619	0.31	2.97
Zone 20	Khanagin Fault	7.3	0.32	4	7.2	1.76	0.16	0.76	0.07	0.764	0.158	2.92
Zone 21	Posht-E Kuh Arc	7.0	0.31	4	6.9	1.86	0.14	0.81	0.06	2.276	0.448	3.60
Zone 22	Kirkuk Embayment	6.6	0.3	4	6.5	1.68	0.17	0.73	0.07	1.022	0.225	2.93
Zone 23	Abdelaziz-Sinjar	5.4	0.36	4	5.2	1.91	0.22	0.83	0.1	0.330	0.108	2.84
Zone 24	Bitilis	6.9	0.32	4	6.8	1.91	0.2	0.83	0.09	1.355	0.308	3.45
Zone 25	Karacadag Extension	6.9	0.31	4	6.8	1.72	0.23	0.75	0.1	0.466	0.122	2.67
Zone 26	East Anatolian Fault	7.8	0.34	4	7.6	2.08	0.12	0.91	0.05	2.125	0.367	3.97
	All Dead Sea	*7.8*	*0.45*	*4*	*7.5*	*2.40*	*0.13*	*1.04*	*0.06*	*4.030*	*0.7*	*4.77*
Zone 27	Ghab Fault	7.5	0.31	4	7.4	1.94	0.14	0.84	0.06	1.009	0.222	3.36
Zone 28	Cyprus	7.1	0.31	4	7.0	2.39	0.12	1.04	0.05	1.982	0.292	4.46
Zone 29	Lebanon Mountain	7.8	0.48	4	7.5	2.11	0.17	0.91	0.07	0.490	0.132	3.33
Zone 30	Palmyra	7.7	0.52	4	7.3	2.23	0.17	1	0.07	0.423	0.105	3.63
Zone 31	Jorden Valley	7.2	0.38	4	7.0	1.86	0.19	0.81	0.08	0.356	0.104	2.79
Zone 32	Carmel Fault	7.0	0.3	4	6.8	2.23	0.23	0.97	0.1	0.002	0	1.59
Zone 33	Sirhan Fault	6.7	0.3	4	6.2	2.23	0.23	0.97	0.1	0.031	0	2.37
Zone 34	Dead Sea Basin	7.8	0.98	4	7.3	2.23	0.19	0.97	0.08	0.216	0.078	3.21
Zone 35	Wadi Araba	7.3	0.3	4	7.0	2.17	0.22	0.94	0.09	0.210	0.08	3.08
Zone 36	Gulf of Aqaba	7.6	0.3	4	7.3	2.48	0.19	1.08	0.08	1.648	0.417	4.54
	All Arabian Shield	*6.5*	*0.41*	*4*	*5.7*	*1.80*	*0.23*	*0.78*	*0.1*	*0.342*	*0.123*	*2.65*
Zone 37	Tabuk	7.6	0.3	4	7.4	2.01	0.22	0.87	0.1	0.118	0.059	2.55
Zone 38	Hijaz	6.2	0.3	4	5.7	1.80	0.23	0.78	0.1	0.102	0	2.13
Zone 39	Jeddah	5.1	0.3	4	4.6	1.80	0.23	0.78	0.1	0.059	0	1.89
Zone 40	Tihama	4.9	0.3	4	4.4	1.80	0.23	0.78	0.1	0.046	0	1.78
Zone 41	Jizan	5.7	0.3	4	5.2	1.80	0.23	0.78	0.1	0.208	0	2.44
Zone 42	Yemen	6.4	0.31	4	6.3	1.97	0.18	0.86	0.08	0.518	0.13	3.15
	All Red Sea	*7.9*	*0.31*	*4*	*7.8*	*1.42*	*0.06*	*0.62*	*0.03*	*12.550*	*1.732*	*3.58*
Zone 43	Southern Red Sea	6.4	0.32	4	6.3	1.90	0.18	0.83	0.08	0.438	0.097	2.96

Table 1 (continued)

Zone No.	Zone Name	M_{max}	σ M_{max}	M_{min}	M_{max}obs	β	σβ	b	σb	λ	σ(λ)	a
Zone 44	Central Red Sea	7.3	0.34	4	7.0	1.58	0.14	0.69	0.06	1.540	0.32	2.95
Zone 45	Transition Red Sea	5.7	0.3	4	5.2	1.61	0.23	0.7	0.1	0.095	0	1.78
Zone 46	Northern Transition Red Sea	6.9	0.31	4	6.8	1.61	0.12	0.72	0.07	0.295	0.031	2.27
Zone 47	Northern Red Sea	6.0	0.3	4	5.5	1.61	0.23	0.7	0.1	0.288	0	2.26
Zone 48	Sinai Triple Junction	6.7	0.14	4	6.6	2.19	0.2	0.95	0.09	1.165	0.356	3.87
	All Aden	*6.7*	*0.12*	*4*	*6.6*	*1.39*	*0.07*	*0.6*	*0.03*	*13.438*	*2.043*	*3.53*
Zone 49	Western Aden	6.7	0.31	4	6.6	1.55	0.09	0.67	0.04	6.222	1.059	3.47
Zone 50	Alula-Fartaq	6.7	0.31	4	6.6	1.15	0	0.5	0.1	2.172	0.397	2.34
Zone 51	Eastern Aden	6.1	0.3	4	6.1	1.15	0	0.5	0.1	4.513	0.793	2.65
Zone 52	Northeastern Aden	6.2	0.48	4	5.8	1.31	0.21	0.57	0.09	0.357	0.13	1.83
	All Owen	*7.2*	*0.12*	*4*	*7.1*	*1.28*	*0.07*	*0.56*	*0.03*	*11.911*	*1.618*	*3.32*
Zone 53	Southern Owen	7.2	0.33	4	7.1	1.31	0.11	0.57	0.05	2.127	0.358	2.61
Zone 54	Owen	6.8	0.24	4	6.5	1.31	0.24	0.57	0.08	0.594	0.16	2.05
Zone 55	Murry Ridge	6.1	0.25	4	5.9	1.15	0	0.5	0.1	0.559	0.193	1.75
Zone 56	Oman Mountains	6.2	0.21	4	6.0	1.94	0.21	0.83	0.09	0.243	0.08	2.71
Zone 57	Arabian Background	6.6	0.31	4	6.5	2.29	0.15	0.99	0.06	2.000	0.342	4.26

Al-Haddad et al. (1994) merge the southernmost section of the Zagros Fold-Thrust Belt with the western side of the Makran Subduction Zone, regardless of the variation in the tectonic regime. Abdalla and Al-Homoud (2004) provided some zones that link the stable Arabian Peninsula with the active areas of the Zagros and Makran, leading to the assumption that earthquakes could uniformly take place inside the Arabian Plate. Tavakoli and Ashtiany (1999) provided a seismic source model that subdivide the Zagros Fold-Thrust Belt into three seismogenic zones, which is too much less than that provided in the current study for this area. For seismic hazard assessment, it is more appropriate to delineate individual faulting structures that responsible for earthquake occurrence. Therefore, the current model is an attempt to provide a higher resolution seismic source model, including the important active structures.

Zahran et al. (2016) provided a source model for the western part of the Arabian Plate. They constrained themselves to the Red Sea escarpment, paying less attention to the small seismic activity reported by the Saudi National Seismic Network (SNSN) directly to the east of their boundaries, the borders of geologic terrains (Fig. 10), surface faulting (Fig. 11), and the occurrence of the historical earthquakes on Ad-Damm Fault (Poirier and Taher 1980). This fault, according to Hamimi et al. (2014), extends to about 42° E, much further inside the Arabian Peninsula than their boundaries. Therefore, the seismic zones No. 40 and 41 of the current model are further extended toward the Arabian shield.

In the near future, the current seismic source model will be used as an alternative model through a logic-tree approach for getting better seismic hazard assessment in the Arabian Plate. It should also note here that continuous updating of different kinds of datasets may permit more accurate delineation of the seismic zones. It is an ongoing process in which continuous improvement of the preceding models should be performed. Future updated databases may confirm the current model or will point out how it should be improved.

References

Abdalla JA, Al-Homoud AS (2004) Seismic hazard assessment of United Arab Emirates and its surroundings. J Earthq Eng 8:817–837

Abdel Rahaman M, Tealeb A, Mohamed A, Deif A, Abou Elenean K, El Hadidy MS (2009) Seismotectonic zones at Sinai and its surrounding. NRIAG J Geophys 1:633–651

Akyuz H, Altunel E, Karabacak V, Yalciner C (2006) Historical earthquake activity of the northern part of the Dead Sea fault zone, southern Turkey. Tectonophysics 426:281–293

Al-Amri A, Punsslan BT, Khalil A, Uy EA (2004) Seismic hazard assessment of western Saudi Arabia and the Red Sea region. IISEE, Japan, pp 95–112

Al-Arifi NS, Fat-Helbary RE, Khalil AR, Lashin AA (2013) A new evaluation of seismic hazard for the northwestern part of Saudi Arabia. Nat Hazards 69:1435–1457

Alavi M (2007) Structures of the Zagros fold-thrust belt in Iran. Am J Sci 307:1064–1095

Alchalabi A, Daoud M, Gomez F, McClusky S, Reilinger R, Abu Romeyeh M, Alsouod A, Yassminh R, Ballani B, Darawcheh R, Sbeinati R, Radwan Y, Al Masri R, Bayerly M, Al Ghazzi R, Barazangi M (2010) Crustal deformation in northwestern Arabia from GPS measurements in Syria: slow slip rate along the northern Dead Sea fault. Geophys J Int 180:125–135

Aldama B (2009) An exploratory study of parameter sensitivity, representation of results and extension of PSHA: case study-United Arab Emirates, PhD thesis, Imperial College London

Aldama B, Bommer JJ, Fenton CH, Staford PJ (2009) Probabilistic seismic hazard analysis for rock sites in the cities of Abu Dhbi, Dubai and Ra's Al Khymah, United Arab Emirates. Georisk 3:1–29

Al-Farajat M, Abdullah D, Al-Adamat R, Al-Amoush H (2016) Geostructural analysis accompanied by GIS vulnerability mapping validated by hydro-chemical modeling in determining spatial expansion of landfills: case study from Jordan. J Civil Eng 10:2016–2367

Al-Haddad M, Siddiqi GH, Al-Zaid R, Arafah A, Necioglu A, Turkelli N (1994) A basis for evaluation of seismic hazard and design criteria for Saudi Arabia. Earthquake Spectra 10:231–258

Allen MB, Talebian M (2011) Structural variation along the Zagros and the nature of the Dezful embayment. Geol Mag 148:911–924

Alridha N, Mohammed H (2015) Seismicity study of Khanaquin area. Iraqi J Sci 56:181–190

Al-Shijbi Y (2013) Probabilistic seismic hazard assessment for Arabian plate. M.Sc. thesis, Sultan Qaboos University, Oman

Al-Zoubi A, Heinrichs T, Sauter M, Qabani I (2006) Geological structure of the eastern side of the lower Jordan Valley/Dead Sea rift: reflection seismic evidence. Mar Pet Geol 23:473–484

Ambraseys NN (1983) Seismicity in the Arab region—an evaluation parameter– AFESD, IDB and UNESCO publication, (abstract)

Ambraseys NN, Jackson JA (1998) Faulting associated with historical and recent earthquakes in the eastern Mediterranean region. Geophys J Int 133:390–406

Ambraseys NN, Melville CP (1982) A history of Persian earthquakes. Cambridge University Press, Cambridge

Ambraseys NN, Melville CP, Adams RD (1994) The seismicity of Egypt, Arabia and Red Sea. Cambridge University Press, Cambridge

ArRajehi A, McClusky S, Reilinger R, Daoud M, Alchalbi A, Ergintav S, Gomez F, Sholan J, Bou-Rabee F, Ogubazghi G, Haileab B, Fisseha S, Asfaw L, Mahmoud S, Rayan A, Bendik R, Kogan L (2010) Geodetic constraints on present-day motion of the Arabian plate: implications for Red Sea and Gulf of Aden rifting. Tectonics 29: TC3011

Asfahani J, Darawcheh R (2017) Seismicity assessment in and around Syria based on instrumental data: application of Gumbel distributions and Gutenberg-Richter relationship. Arab J Geosci 10:86

Authemayou C, Bellier O, Chardon D, Mal-Ekzadeh Z, Abbassi M (2005) Active partitioning between strike-slip and thrust faulting in the Zagros fold-and-thrust belt (southern Iran). C R Geosci 337: 539–545

Babiker N, Mula A, El-Hadidy S (2015) A unified mw-based earthquake catalogue and seismic source zones for the Red Sea. J Afr Earth Sci 109:168–176

Bachmanov D, Trifonov V, Hessami K, Kozhurin A, Ivanova T, Rogozhin E, Hademi M, Jamali F (2004) Active faults in the Zagros and Central Iran. Tectonophysics 380:221–241

Baer G, Funning G, Shamir G, Wright T (2008) The 1995 November 22, Mw 7.2 Gulf of Elat earthquake cycle revisited. Geophys J Int 175: 1040–1054

Baker C, Jackson J, Priestley K (1993) Earthquakes on the Kazerun line in the Zagros Mountains of Iran: strike-slip faulting within a fold-and-thrust belt. Geophys J Int 115:41–61

Bartov Y, Steinitz G, Eyal M, Eyal Y (1980) Sinistral movement along the Gulf of Aqaba—its age and relation to the opening of the Red Sea. Nature 285:220–222

Bayrak Y, Öztürk AS, Çınara H, Kalafat D, Tsapanos TM, Koravos GC, Leventakis GA (2009) Estimating earthquake hazard parameters from instrumental data for different regions in and around Turkey. Eng Geol 105:200–210

Ben Avraham Z, Almajor G, Garfunkel Z (1979) Sediments and structure of the Gulf of Eilat, northern Red Sea. Sediment Geol 23:239–267

Ben Menahem A (1979) Earthquake catalogue for the Middle East. Boll Geofis Teor Appl 21: 245–310

Berberian M (1981) Active faulting and tectonics of Iran, in Gupta, H.K., and Delany, F.M., editors, Zagros-Hindu Kush-Himalaya geodynamic evolution: American Geophysical Union geodynamic series 3, 33–69

Berberian M (1995) Master 'blind' thrust faults hidden under the Zagros folds, active basement tectonics and surface morphotectonics. Tectonophysics 241:193–224

Berberian M, Yeats RS (1999) Patterns of historical earthquake rupture in the Iranian plateau. Bull Seismol Soc Am 89:120–139

Bosence D, Nichlos G, Al-Subbary A, Al-Thour K, Reeder M (1996) Synrift continental to marine depositional sequences, tertiary, Gulf of Aden, Yemen. J Sediment Res 66:766–777

Bosworth W, Huchon P, McClay K (2005) The Red Sea and the Gulf of Aden basins. J Afr Earth Sci 43:334–378

Brew, G., 2001. Tectonic evolution of Syria interpreted from integrated geophysical and geological analysis. [PhD thesis] Cornell Univ, USA

Brew G, Barazangi M, Al-maleh A, Sawaf T (2001) Tectonic and geologic evolution of Syria. GeoArabia 6:573–616

Bulut F, Marco B, Tuna E, Janssen C, Kılıç T, Dresen G (2012) The East Anatolian Fault Zone: seismotectonic setting and spatiotemporal characteristics of seismicity based on precise earthquake locations. J Geophys Res 117:B07304

Byrne DE, Sykes LR, Davis DM (1992) Great thrust earthquakes and aseismic slip along the plate boundary of the Makran subduction zone. J Geophys Res 97:449–478

Camp VE (1984) Island arcs and their role in the evolution of the western Arabian Shield. Bull Geol Soc Am 95:913–921

Cochran JR, Martinez F, Steckler MS, Hobart MA (1986) Conrad deep, a new northern Red Sea deep, origin and implications for continental rifting. Earth Planet Sci Lett 78:18–32

Coleman RG (1993) geologic evolution of the Red Sea. Oxford monographs on geology and geophysics, 24. Oxford University Press, Oxford

Cornell CA, Vanmarcke EH (1969) The major influences on seismic risk. In: Proceedings of the fourth world conference of earthquake engineering, 1. Santiago, Chile, pp 69–83

Daeron M, Benedetti L, Tapponnier P, Sursock A, Finkel RC (2004) Constraints on the post-25-ka slip rate of the Yammouneh fault (Lebanon) using in situ cosmogenic Cl-36 dating of offset limestone-clast fans. Earth Planet Sci Lett 227:105–119

Daeron M, Klinger Y, Tapponnier P, Elias A, Jacques E, Sursock A (2007) 12,000 year long record of 10 to 13 paleo-earthquakes on the Yammouneh fault (Levant fault system, Lebanon). Bull Seismol Soc Am 97:749–771

Daggett P, Morgan P, Boulos FK, Hennin SF, El-Sherif AA, El-Sayed AA, Basta NZ, Melek YS (1986) Seismicity and active tectonics of the Egyptian Red Sea margin and the northern Red Sea. Tectonophysics 125:313–324

Deif A, El-Hussain I (2012) Seismic moment rate and earthquake mean recurrence interval in the major tectonic boundaries around Oman. J Geophys Eng 9:773–783

Deif A, Abou-Elenean K, El-Hadidy M, Tealeb A, Mohamed A (2009a) Probabilistic seismic hazard maps for Sinai Peninsula, Egypt. J Geophys Eng 6:288–297

Deif A, Zahran HM, El-Hadidy MS, Bawajee AO, El-Hadidy SY, Mansoub TA (2009b) Seismic hazard assessment along Haramein high speed rail project (Makkah-Madinah), internal SGS report

Deif A, Al-Shijbi Y, El-Hussain I, Ezzelarab M, Mohamed AME (2017) Compiling an earthquake catalogue for the Arabian plate, western Asia. J Asian Earth Sci 147:345–375

DeMets C, Gordon RG, Argus DF, Stein S (1990) Current plate motions. Geophys J Int 101:425–478

El-Hadidy SY (2015) Seismicity and seismotectonic setting of the Red Sea and adjacent areas. In: Rasul NMA, Stewart ICF (eds) The Red Sea. Springer Earth System Sciences, Berlin Heidelberg, pp 151–159

El-Hefnawy M, Deif A, El-Hemamy ST, Gomaa NM (2006) Probabilistic assessment of earthquake hazard in Sinai in relation to the seismicity in the eastern Mediterranean region. Bull Eng Geol Environ 65:309–319

El-Hussain I, Deif A, Al-Jabri K, Al-Hashmi S, Al-Toubi K, Al-Shijbi Y, Al-Saifi M (2010) Probabilistic and deterministic seismic hazard assessment for Sultanate of Oman (phase I), project #22409017, submitted to Sultan Qaboos University, Oman

El-Hussain I, Deif A, Al-Jabri K, Toksoz N, El-Hady S, Al-Hashmi S, Al-Toubi K, Al-Shijbi Y, Al-saifi M, Kuleli S (2012) Probabilistic seismic hazard maps for Sultanate of Oman. Nat Hazards 64:173–210

El-Isa Z (2015) Seismicity and seismotectonics of the Red Sea region. Arab J Geosci 8:8505–8525

El-Isa ZH, Al-Shanti A (1989) Seismicity and tectonics of the Red Sea and western Arabia. Geophys J 97:449–457

Falcon NL (1961) Major earth-flexing in the Zagros Mountains of Southwest Iran. Q J Geol Soc Lond 117:367–376

Farhoudi G, Karig DE (1977) Makran of Iran and Pakistan as an active arc system. Geology 5:664–668

Ferry M, Meghraoui M, Abou Karaki N, Al-Taj M, Khalil L (2011) Episodic behavior of the Jordan Valley section of the Dead Sea fault from a 14-kyr-long integrated catalogue of large earthquakes. Bull Seismol Soc Am 101:39–67

Fouad SFA, Sissakian VK (2011) Tectonic and structural evolution of the Mesopotamia plain. Iraqi Bull Geol Mining, Spec Issue 4:33–46

Fournier M, Chamot-Rooke N, Petit C, Fabbri O, Huchon P, Maillot B, Lepvrier C (2008) In-situ evidence for dextral active motion at the Arabia-India plate boundary. Nat Geosci, Nature Publishing Group 1:54–58

Garfunkel Z (1970) The tectonic of the western margin of the southern Arava (in Hebrew, English summary), thesis. Hebrew University, Jerusalem

Garfunkel Z, Zak I, Freund R (1981) Active faulting in the Dead Sea rift. Tectonophysics 80:1–26

Gillard D, Wyss M (1995) Comparison of strain and stress tensor orientation: application to Iran and southern California. J Geophys Res 100:22197–22213

Girdler RW, Styles P (1974) Two stages Red Sea floor spreading. Nature 247:7–11

Girdler RW, Underwood M (1985) The evolution of early oceanic lithosphere in the southern Red Sea. Tectonophysics 116:95–108

Gok R, Mahdi H, Al-Shukri H, Rodgers AJ (2008) Crustal structure of Iraq from receiver functions and surface wave dispersion: implications for understanding the deformation history of the Arabian–Eurasian collision. Geophys J Int 172:1179–1187

Gomez F, Meghraoui M, Darkal AN, Hijazi F, Mouty M, Suleiman Y, Sbeinati R, Darawcheh R, Al-Ghazzi R, Barazangi M (2003) Holocene faulting and earthquake recurrence along the Serghaya branch of the Dead Sea fault system in Syria and Lebanon. Geophys J Int 153:658–674

Gomez F, Karam G, Khawlie M, McClusky S, Vernant P, Reilinger R, Jaafar R, Tabet C, Khair K, Barazangi M (2007) Geophys J Int 168: 1021–1028. Global Positioning System measurements of strain accumulation and slip transfer through the restraining bend along the Dead Sea fault system in Lebanon

Greenwood WR, Anderson RE, Fleck RJ, Roberts RJ (1980) Precambrian geologic history and plate tectonic evolution of the Arabian shield. Saudi Arabian Directorate General of Mineral Resources, Bulletin 24

Grunthal G, Wahlstrom R (2012) The European-Mediterranean earthquake catalogue (EMEC) for the last millennium. J Seismol 16: 535–570

Gullen L, Pinar A, Kalafat D, Ozel N, Horasan G, Yilmazer M, Isikar A (2002) Surface fault breaks, aftershock distribution, and rupture process of the 17 August 1999, Izmit earthquakes. Bull Seismol Soc Am 92:230–244

Gutenberg B, Richter CF (1956) Magnitude and energy of earthquakes. Ann Geofis 9:1–15

Haghipour A, Chorashi M, Kadjar M (1984) Explanatory text of the seismotectonic map of Iran, Afghanistan and Pakistan, commission for geological map of world-UNESCO. Geological Survey of Iran, Tehran

Hamimi Z, El-Sawy K, El-Fakharani A, Matsah M, Shujoon A, El-Shafei MK (2014) Neoproterozoic structural evolution of the NE-trending Ad-Damm Shear Zone, Arabian Shield, Saudi Arabia. J Afr Earth Sci 99:51–63

Heidarzadeh M, Satake K (2014) Possible sources of the tsunami observed in the northwestern Indian Ocean following the 2013 September 24 Mw 7.7 Pakistan inland earthquake. Geophys J Int 199:752–766

Hessami K, Koyi H, Talbot C (2001) The significance of the strike-slip faulting in the basement of the Zagros fold and Thrust Belt. J Pet Geol 24:5–28

Hessami K, Jamali F, Tabassi H (2003) Major active faults in Iran. Ministry of Science, research and technology, International Institute of Earthquake Engineering and Seismology (IIEES), 1: 250000 scale map

Hessami K, Nilforoushan F, Talbot CJ (2006) Active deformation within the Zagros Mountains deduced from GPS measurements. J Geol Soc 163:143–148

Hoffmann G, Klaus R, Christoph G, Magdalena R, Frank Preusser (2013) Holocene tsunami history of the Makran Subduction Zone (Northern Indian Ocean). 4th International INQUA Meeting on Paleoseismology, Active Tectonics and Archeoseismology (PATA), 9–14 October 2013, Aachen, Germany

Hofstetter R, Klinger Y, Amrat AQ, Rivera L, Dorbath L (2007) Stress tensor and focal mechanisms along the Dead Sea fault and related structural elements based on seismological data. Tectonophysics 429:165–181

Huber H (1977) Geological map of Iran, 1:1,000,000 with explanatory note, Natl. Iran Oil Co. Exploration and Production Affairs, Tehran

Ibrahim AO (2009) Tectonic Style and Evolution of the NW Segment of the Zagros Fold-Thrust Belt, Sulaimani Governorate, Kurdistan Region, NE Iraq. Ph.D. thesis, University of Sulaimani, Sulaimani

Jackson JA, McKenzie D (1984) Active tectonics of the Alpine-Himalayan Belt between western Turkey and Pakistan. Geophys J R Astron Soc 77:185–264

Jackson JA, White NJ, Garfunkel Z, Anderson H (1988) Relations between normal-fault geometry, tilting, and vertical motions in extensional terrains, an example from the southern Gulf of Suez. J Struct Geol 10:155–170

Johnson PR (1998) Tectonic map of Saudi Arabia and adjacent areas. Deputy Ministry for Mineral Resources, USGS TR-98-3, Saudi Arabia

Johnson PR, Kattan FH (2012) The geology of the Saudi Arabian Shield. Jeddah, Saudi Geological Survey

Johnson PR, Woldehaimanot B (2003) Development of the Arabian-Nubian Shield: perspectives on accretion and deformation in the northern east African Orogen and the assembly of Gondwana. Geol Soc Lond, Spec Publ 206:289–325

Johnson PR, Andersen A, Collins AS, Fowler AR, Fritz H, Ghebreab W, Kusky T, Stern RJ (2011) Late Cryogenian–Ediacaran history of the Arabian–Nubian Shield: a review of depositional, plutonic, structural, and tectonic events in the closing stages of the northern East African Orogen. J Afr Earth Sci 10:1–179

Kazmin VG (2002) The late Paleozoic to Cainozoic in-traplate deformation in North Arabia: a response to plate boundary-forces. European

Geosciences Union (EGU). Stephan Mueller Spec Publ Ser 2:123–138
Kijko A (2004) Estimation of the maximum earthquake magnitude Mmax. Pure Appl Geophys 161:1655–1681
Kijko A, Sellevoll MA (1992) Estimation of earthquake hazard parameters from incomplete data files, part II. Bull Seismol Soc Am 82: 120–134
Kijko A, Singh M (2011) Statistical tools for maximum possible earthquake magnitude estimation. Acta Geophysica 59:674–700
Klinger Y, Avouac JP, Dorbath L, Abou Karaki N, Tisnerat N (2000) Seismic behaviour of the Dead Sea fault along Araba valley, Jordan. Geophys J Int 142:769–782
Klinger Y, Le Béon M, Al-Qaryouti M (2015) 5000 yr of paleoseismicity along the southern Dead Sea fault. Geophys J Int 202:313–327
Kusky T, Robinson C, El-Baz F (2005) Tertiary-Quaternary faulting and uplift in the northern Oman Hajar Mountains. J Geol Soc 162:871–888
Lazar M, Ben-Avraham Z, Marco S, Garfunkel Z, Porat N, Ben-Avraham Z (2010) Is the Jericho escarpment a tectonic or a geomorphological feature? Active faulting and paleoseismic trenching. J Geol 118: 261–276
Le Beon M, Klinger Y, Al-Qaryouti M, Meriaux AS, Finkel RC, Elias A, Mayyas O, Ryerson FJ, Tapponnier P (2010) Early Holocene and Late Pleistocene slip rates of the southern Dead Sea fault determined from be-10 cosmogenic dating of offset alluvial deposits. J Geophys Res Solid Earth 115(B11414):24
Lees GM, Falcon NL (1952) The geographical history of the Mesopotamian plains. Geogr J 118:24–39
Lorei S, Lucazeau F, d'Acremont E, Watremez L, Autin J, Rouzo S, Bellahsen N, Tiberi C, Ebinger C, Beslier MO, Perrot J, Razin P, Rolandone F, Sloan H, Stuart G, Al Lazki A, Al-Toubi K, Bache F, Bonneville A, Goutorbe B, Huchon P, Unternehr P, Khanbari K (2010) Contrasted styles of rifting in the eastern Gulf of Aden: a combined wide-angle, multichannel seismic, and heat flow survey. Geochem Geophys Geosyst 11:1–14
Marco S, Klinger Y (2014) Review of on-fault palaeosismic studies along the Dead Sea fault, chapter 6, in Dead Sea transform fault system: reviews: 183–205, editors Garfunkel Z, Ben Avraham Z and Kagan E, Springer
Marco S, Rockwell T, Heimann A, Frieslander U (2005) Late Holocene activity of the Dead Sea transform revealed in 3D paleoseismic trenches on the Jordan Gorge segment. Earth Planetary Science Letters 234:189–205
Masson F, Hamiel Y, Agnon A, Klinger Y, Deprez A (2015) Variable behavior of the Dead Sea Fault along the southern Araba segment from GPS measurements. C R Geosci 347:161–169
McClusky S, Reilinger R, Mahmoud S, Ben Sari D, Tealeb A (2003) GPS constraints on Africa (Nubia) and Arabia plate motions. Geophys J Int 155:126–138
Meghraoui, M. (2015) Paleoseismic history of the Dead Sea fault zone. In Encyclopedia of Earthquake Engineering: https://doi.org/10.1007/978-3-642-36197-5_40-1
Merghelani H M (1981) Seismicity of the Yanbu region Kingdom of Saudi Arabia. U.S. Geological survey, Saudi Arabia project report 371, technical records 16
Mokhtari M, Fard I, Hessami K (2008) Structural elements of the Makran region, Oman Sea and their potential relevance to tsunamigenisis. Nat Hazards 47:185–199
Mooney W, Gettings ME, Blank HR, Healy JH (1985) Saudi Arabian seismic deep refraction profile: a travel time interpretation of crustal and upper mantle structure. Tectonophysics 111:173–246
Musson RMW (2009) Subduction in the western Makran: the historian's contribution. J Geol Soc, Lond 166:387–391
Nemer T, Meghraoui M (2006) Evidence of coseismic ruptures along the Roum fault (Lebanon): a possible source for the AD 1837 earthquake. J Struct Geol 28:1483–1495
Nemer T, Gomez F, Al Haddad S, Tabet C (2008) Coseismic growth of sedimentary basins along the Yammouneh strike-slip fault (Lebanon). Geophys J Int 175:1023–1039
Niemi TM, Zhang H, Atallah M, Harrison JBJ (2001) Late Pleistocene and Holocene slip rate of the northern Wadi Araba fault, Dead Sea transform, Jordan. J Seismol 5:449–474
Onur T, Gok R, Abdulnaby W, Mahdi H, Numan NMS, Al-Shukri H, Shakir AM, Chlaib HK, Ameen TH, Abd NA (2017) A comprehensive earthquake catalogue for Iraq in terms of moment magnitude. Seismol Res Lett, Online Publ 88:798–811
Page WD, Anttonen G, Latham GV (1978) The Makran coast of Iran, a possible seismic gap, proceedings of conference VI: methodology for identifying seismic gaps and soon-to-break gaps. USGS Open file report 78-943:611–634
Palano M, Paola Imprescia P, Gresta S (2013) Current stress and strain-rate fields across the Dead Sea fault system: constraints from seismological data and GPS observations. Earth Planet Sci Lett 369–370:305–316
Pallister JS (1984) Explanatory notes to the geologic map of Al Lith quadrangle, sheet 20 MD, Kingdom of Saudi Arabia: Saudi Arabia Deputy Ministry for mineral resources, Open File Report USGS-OF-04-8
Pararas-Carayannis G (2004) Seismo-dynamics of compressional tectonic collision-potential for tsunami genesis along boundaries of the Indian, Eurasian and Arabian plates. Abstract submitted to the international conference HAZARDS, Hyderabad, India, 2-4 Dec. 2004
Peyret DY, Hessami K, Regard V, Bellier P, Vernant P, Daigni'eres M, Nankali H, Van Gorp S, Goudarzi M, Ch'ery J, Bayer R, Rigoulay M (2009) Present-day strain distribution across the Minab-Zendan-Palami fault system from dense GPS transects. Geophys J Int 179: 751–762
Poirier JP, Taher MA (1980) Historical seismicity in the near and Middle East, North Africa, and Spain from Arabic documents (VIIth-XVIIth century). Bull Seismol Soc Am 70:2185–2201
Quittmeyer RC (1979) Seismicity variations in the Makran region of Pakistan and Iran: relation to great earthquakes. Pure Appl Geophys 117:1212–1228
Ramsay CR, Drysdall AR, Clark MD (1986) Felsic plutonic rocks of the Midyan region, Kingdom of Saudi Arabia—I, distribution, classification, and resource potential, In, Drysdall AR, Ramsay CR, and Stoeser DB (eds), Felsic plutonic rocks and associated mineralization of the Kingdom of Saudi Arabia. Saudi Arabian deputy ministry for mineral resources bulletin 29: 63–77
Rasul NMA, Stewart ICF, Nawab ZA (2015) Introduction to the Red Sea: its origin, structure, and environment: in Rasul NMA, Stewart CF (eds) the Red Sea. Springer Earth System Sciences, Berlin, Heidelberg, pp 1–28
Regard V, Bellier O, Thomas J-C, Bourl'es D, Bonnet S, Abbassi MR, Braucher R, Mercier J, Shabanian E, Soleymani SH, Feghhi KH (2005) Cumulative right-lateral fault slip rate across the Zagros-Makran transfer zone: role of the Minab-Zendan fault system in accommodating Arabia-Eurasia convergence in Southeast Iran. Geophys J Int 162:177–203
Reilinger R, McClusky S, Vernant P, Lawrence S, Ergentav S, Cakmak R, Ozener H, Kadirov F, Guliev I, Stepanyan R, Nadariya M, Hahubia G, Mahmoud S, Sakr K, ArRajehi A, Paradissis D, Al-Aydrus A, Prilepin M, Guseva T, Evren E, Dmitrotsa A, Filikov SV, Gomez F, Al-Ghazzi R, Karam G (2006) GPS constraints on continental deformation in the Africa-Arabia-Eurasia continental collision zone and implications for the dynamics of plate interactions. J Geophys Res 111:B05411
Roobol MJ, Stewart ICF (2009) Cenozoic faults and recent seismicity in northwest Saudi Arabia and the Gulf of Aqaba region. Saudi Geological Survey Technical Report SGSTR-2008-7
Sadeh M, Hamiel Y, Ziv A, Bock Y, Fang P, Wdowinski S (2012) Crustal deformation along the Dead Sea transform and the Carmel Fault

inferred from 12 years of GPS measurements. J Geophys Res 117: B08410

Salamon A, Avraham H, Garfunkel Z, Ron H (2003) Seismotectonics of Sinai subplate-eastern Mediterranean region. Geophys J Int 155: 149–173

Shearman DJ (1977) The geological evolution of southern Iran, the report of the Iranian Makran expedition. Geogr J 142:393–410

Sneh A (1996) The Dead Sea rift: lateral displacement and down faulting phases. Tectonophysics 263:277–292

Stoneley R (1974) Evolution of the continental margins bounding a former Tethys. In: Burk CA, Drake CL (eds) The geology of continental margins. Springer, New York, pp 889–903

Sykes LR, Seeber L (1982) Great earthquakes and great asperities along the San Andreas fault, southern California (Abs.), EOS. Trans Am Geophys Union 63:1030–1041

Talebian M, Jackson J (2004) A reappraisal of earthquake focal mechanisms and active shortening in the Zagros mountains of Iran. Geophys J Int 156:506–526

Tamsett D, Searle R (1990) Structure of Alula-Fartak fracture zone, Gulf of Aden. J Geophys Res 95:1239–1254

Tavakoli B, Ashtiany MG (1999) Seismic hazard assessment of Iran. Ann Di Geofisica 42:1013–1021

Tavakoli F, Walpersdorf A, Authemayou C, Nankali HR, Hatzfeld D, Tatar M, Djamour Y, Nilforoushan F, Cotte N (2008) Distribution of the right-lateral strike–slip motion from the main recent fault to the Kazerun fault system (Zagros, Iran): evidence from present-day GPS velocities. Earth Planet Sci Lett 275:342–347

Vermeulen P, Kijko A (2017) More statistical tools for maximum possible earthquake magnitude estimation. Acta Geophys, Publ Online 65: 579–587. https://doi.org/10.1007/s11600-017-0048-3

Vernant PH, Nilforoushan F, Hatzfeld D, Abassi MR, Vigny C, Masson F, Nankali H, Martinod J, Ashtiani A, Bayer R, Tavakoli F, Chery J (2004) Present-day crustal deformation and plate kinematics in Middle East constrained by GPS measurements in Iran and northern Oman. Geophys J Int 157:381–398

Wetzler N, Marcos S, Heifetz E (2010) Quantitative analysis of seismogenic shear-induced turbulence in lake sediments. Geology 38:303–306

Xu W, Dutta R, Johnsson S (2015) Identifying active faults by improving earthquake locations with InSAR data and Bayesian estimation: the 2004 Tabuk (Saudi Arabia) earthquake sequence. Bull Seismol Soc Am 105:765–775

Yamini-Fard F, Hatzfeld D, Farahbod AM, Paul A, Mokhtari M (2007) The diffuse transition between the Zagros continental collision and the Makran oceanic subduction (Iran): microearthquake seismicity and crustal structure. Geophys J Int 170:182–194

Zahran HM, Sokolov V, Roobol J, Stewart ICF, El-Hadidy SY, El-Hadidy M (2016) On the development of a seismic source zonation model for seismic hazard assessment in western Saudi Arabia. J Seismol 20:747–769

Zilberman E, Amit R, Porat N, Enzel Y, Avner U (2005) Surface ruptures induced by the devastating 1068 AD earthquake in the southern Arava valley, Dead Sea rift, Israel. Tectonophysics 408:79–99